BRL

TECHNICAL NOTE NO. 1533
APRIL 1964

BLAST PATTERNS IN COMPLEX TUNNEL MODELS

George D. Teel

BALLISTIC RESEARCH LABORATORIES

ABERDEEN PROVING GROUND, MARYLAND

The findings in this report are not to be construed as an official Department of the Army position.

BLANK PAGES
IN THIS
DOCUMENT
WERE NOT
FILMED

B A L L I S T I C R E S E A R C H L A B O R A T O R I E S

TECHNICAL NOTE NO. 1533

APRIL 1964

BLAST PATTERNS IN COMPLEX TUNNEL MODELS

Ge ·ge D. Teel

Terminal Ballistics Laboratory

A B E R D E E N P R O V I N G G R O U N D, M A R Y L A N D

B A L L I S T I C R E S E A R C H L A B O R A T O R I E S

TECHNICAL NOTE NO. 1533

GDTeel/idk
Aberdeen Proving Ground, Md.
April 1964

BLAST PATTERNS IN COMPLEX TUNNEL MODELS

ABSTRACT

The Ballistic Research Laboratories detonation-driven shock tube was utilized to expose four complex tunnel models to high pressure blast waves. The models were exposed to shock pressures of 200, 500, and 800 psi. The data obtained from the shock tube tests were reduced, plotted, and extrapolated to give expected values for the models when exposed to a 1500 psi shock wave from a 10 megaton nuclear weapon.

TABLE OF CONTENTS

LIST OF FIGURES AND TABLES

LIST OF FIGURES AND TABLES (CONT'D)

INTRODUCTION

In March 1963, the Ballistic Research Laboratories' Shock Tube Facility initiated a program to test a series of model underground tunnel configurations. The work was performed at the request of and funded by Bureau of Yards & Docks, U. S. Navy in response to letter 74B/JMC:JS of 6 March 1963. It was requested that the models be subjected to an input shock wave the equivalent of a 1500 psi wave from a 10 megaton nuclear weapon and that pressure-time records be made at specific positions within the models. The physical characteristics of the shock tube precluded the possibility of conducting the tests at the desired pressure. Therefore, modifications were made on the shock tube to permit the tests to be conducted with input pressures up to 800 psi and to obtain data that would permit extrapolation to the desired level.

The four models, Fig. 1 - 4, were attached to the moving test section, Fig. 5, as shown in the photograph in Fig. 6. The models thus oriented were exposed face-on to shock waves up to 160 psi. Previous experiments at BRL have shown that a 160 psi shock will transmit a 200 psi shock wave into a tunnel oriented face-on to the blast wave and surrounded by a baffle that can be considered infinite and similarly that an 800 psi shock wave will transmit a 200 psi shock wave into a tunnel oriented side-on to the blast wave. Consequently this exposure, face-on to 160 psi shock wave, was considered equivalent to an 800 psi shock wave side-on to the models.

The indicated gage positions were instrumented with piezo electric transducers and recorded with oscillographic equipment. Fig. 7 is a tracing of a typical record thus obtained.

PROCEDURE

The models were exposed separately to each of three input shock pressures, equivalent to 200, 500, and 800 psi side-on to the entrances. In all cases pressure-time records were taken for all gage positions simultaneously. A zero-time mark was included on all recording channels to provide time correlation and arrival times, with respect to shock arrival at the tunnel entrance for each gage position. Each gage was dynamically calibrated before and after each shot and the pre- and post-shot calibrations were averaged (if variations occurred) to obtain the pressure values from the records. A 1,000 cycle/second timing mark was provided on the film to yield time for the recordings.

RESULTS

The reduction of the pressure-time records involved the determination of a number of various values from the data. The pressure initially recorded by the gage, that is the first step, was measured along with the arrival time for that pressure. The pressure was calculated by means of the simple proportion between the known calibration pressure and the height of the calibration step on the film and the height of the actual shock wave step. The arrival time was measured from the records using the zero-time mark. The zero-time or fiducial mark was a pulse simultaneously imposed on all data channels. By measuring the time separation, using the 1,000 cycle/second timing marks, between each zero-time mark and the arrival of the shock for all data channels and subtracting from each data channel in the model, the time separation of the input channel, the time required for the transmitted shock wave to travel from the entrance to the gage position was obtained. Assuming then that zero-time is the arrival of the input shock wave at the model entrance, the arrival time for all gage positions is known.

The pressure profiles, such as those in Fig. 7, were then approximated as closely as possible by a series of straight lines. The pressure and time was then determined for each end of each of the straight line approximations. All actual recorded times were then scaled up to real times with respect to the full-scale prototypes, that is, multiplied by the scale factor of 32. This yielded then a series of pressure-time values of real pressure and times that would be obtained in the full scale case.

Because the shock tube did not exactly reproduce its pressure from shot to shot, the data obtained for the various models were not all for the same input pressures. Consequently, it was decided to normalize the data with respect to the input pressures to allow them to be plotted at the same pressures and to provide correlation between the predictions and the recorded data. This normalized data along with the full scale times were then plotted. Fig. 8 - 22 are plots of this pressure-time data along with a plot of the wave shape from a 10 megaton nuclear weapon.

The 10 megaton wave shape was obtained by scaling the 1 kiloton data from the IBM Problem "M". Since the shock tube produced a wave shape equivalent to a much larger yield than the 10 megaton weapon, the applied pressure remained higher for a longer time than would be encountered in the actual case. Once the shock wave has been transmitted through the model, the pressure would then begin to rise as the model filled, much as a chamber, until an equilibrium was reached between

the outside pressure and the pressure within the model. This filling would be expected in either the shock tube test or the actual field case, but the extent of filling would be determined by the waveshape of the input shock wave. It is reasonable to assume therefore, that the ultimate or maximum pressure obtained for each gage position would be less for a 10 megaton wave shape than for the wave shape from a much larger yield.

When the pressure-time record (measured) from a particular gage position crossed the pressure-time profile of the 10 megaton weapon (scaled from IBM Problem "M"), it was assumed that an equilibrium condition existed between that gage position and the input wave. At this point the pressure-time profile at the gage position would continue as observed in the shock tube test (overshoot the 10 megaton wave shape) until a rarefaction wave moving at the local speed of sound could travel from the entrance to the gage position and relieve the pressure to that of the outside. The time for the rarefaction wave to travel to the gage position was calculated for each of the records and the observed pressure-time profile was continued, past the equilibrium point, for that time. At this time of relief, the pressure at the gage position would begin to decay at some rate greater than that of the outside wave shape so that the pressure in the model would approach that of the outside. Lack of information as to the rate of this decay however, prohibits an approximation of the wave shape past the time of the relief.

A number of values of pressure and time are available from these plots (Fig 8 - 22). For the three input shock pressures the following values are available, for each gage position of each model, (1) the initial pressure step at the gage position, (2) the time of arrival of this initial step, (3) the pressure at the time of the relief due to the rarefaction, and (4) the time at which the relief will occur.

Since the data were taken at 200, 500, and 800 psi as opposed to the point of interest, 1500 psi, the data had to be extrapolated to the higher pressure. This was accomplished by plotting the input pressure versus the initial pressure, the arrival time, etc. for each position in each model and extrapolating these curves to 1500 psi (see Fig. 23 - 38).

The data plotted on Fig. 23 - 38 and that read from the extrapolation of these curves are listed in Table 1. The table gives for each position of each model, the values of initial pressure, arrival time at the gage position, the

pressure at the time of relief, and the time of the relief for input pressures of 200, 500, 800, and 1500 psi. In addition if a pressure exceeding that observed at the time of rarefaction occurred on the pressure-time records, that pressure and the time of its occurrence is listed.

Since the models were designed to be oriented side-on to the blast wave, rather than the face-on configuration used, one point should be mentioned. Fig. 23 indicates a high pressure at position 2 of Model 1. This is probably due to some extent to the simultaneous arrival and interaction of the three shock waves, transmitted from the three entrances. Since in the true case the shock arrival at the entrances would be different due to the varying ground ranges of the entrances, the transmitted shocks would not arrive at the intersection simultaneously. This discrepancy, between simultaneous and non-simultaneous arrival at the intersection would effect the shock interactions and hence, should be considered when using information taken from Model 1.

ACKNOWLEDGEMENTS

The author wishes to express his appreciation to W. T. Matthews for his assistance in gathering the data for this report.

George D. Teel

GEORGE D. TEEL

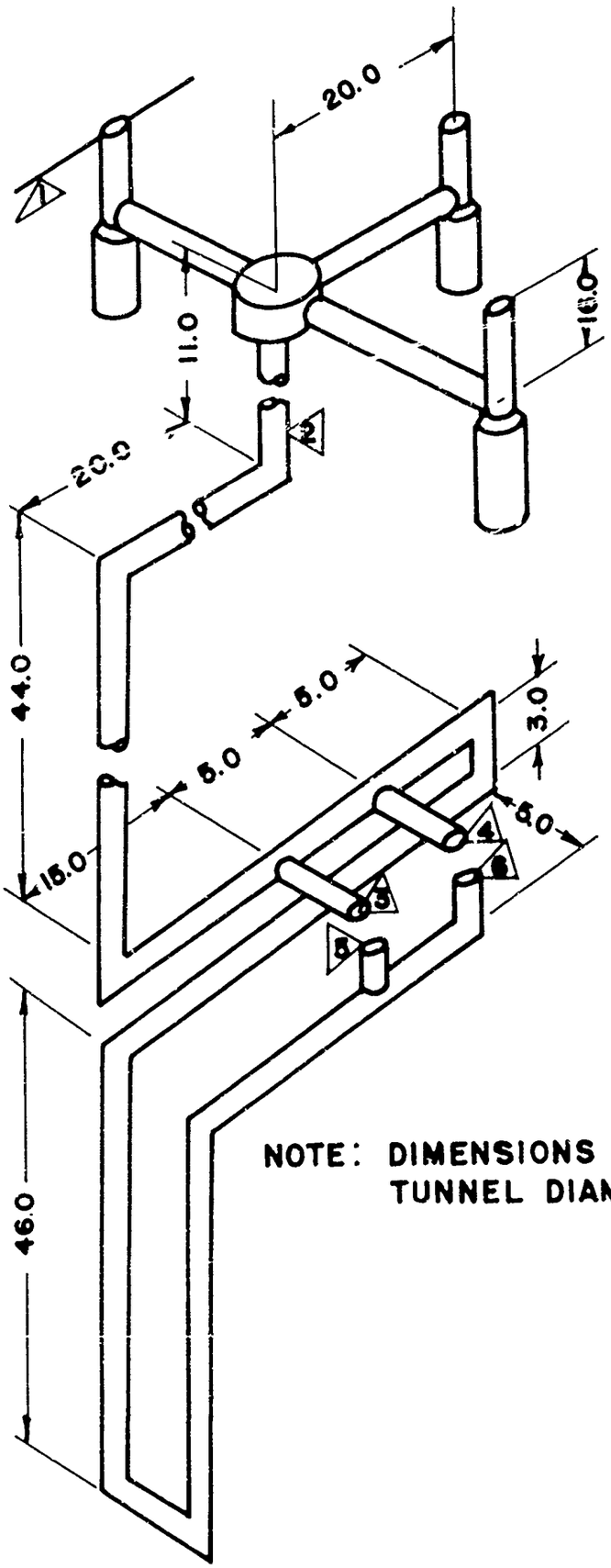

NOTE: DIMENSIONS ARE IN TUNNEL DIAMETERS

FIG. 1 MODEL # 1

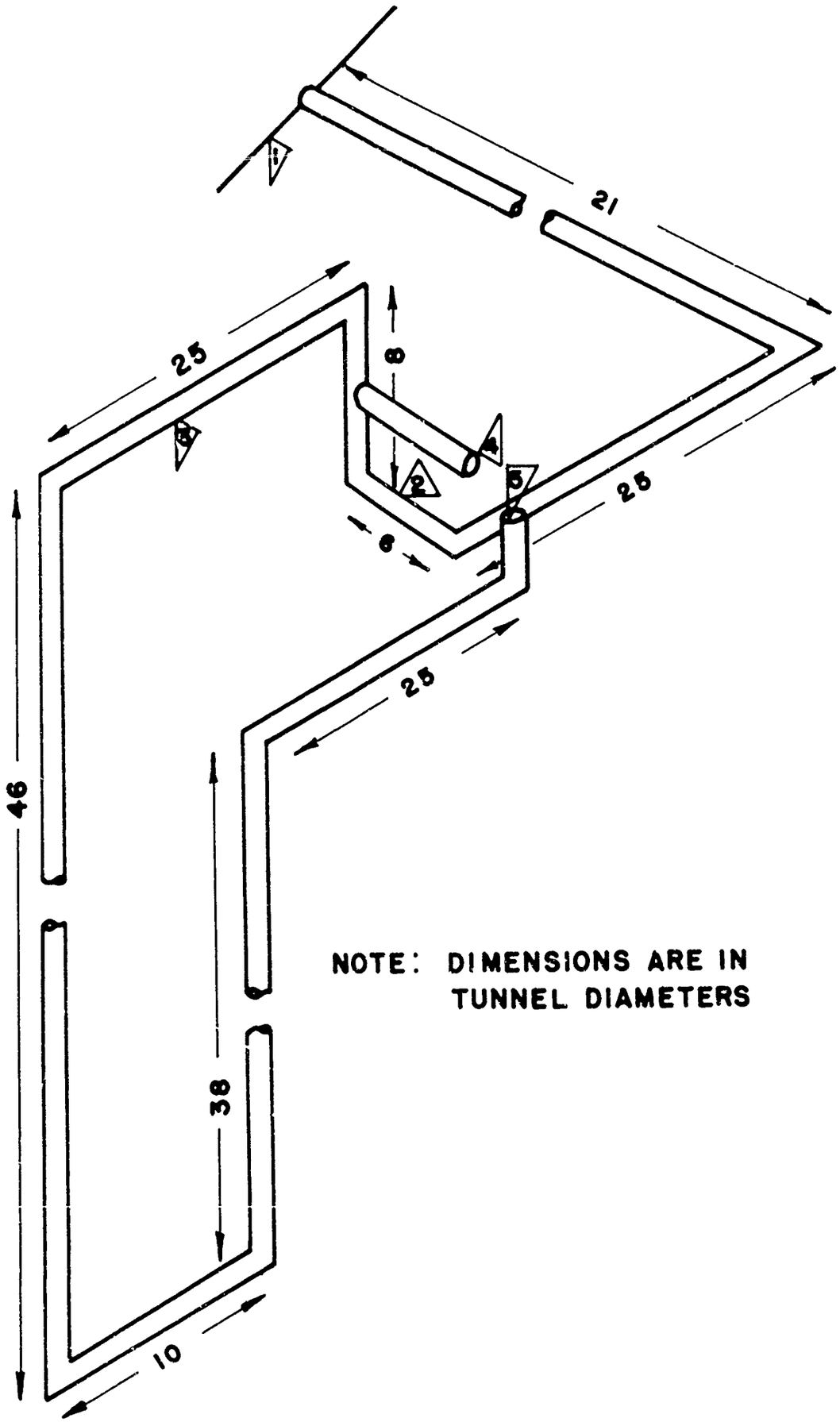

NOTE: DIMENSIONS ARE IN TUNNEL DIAMETERS

FIG. 2 MODEL # 2

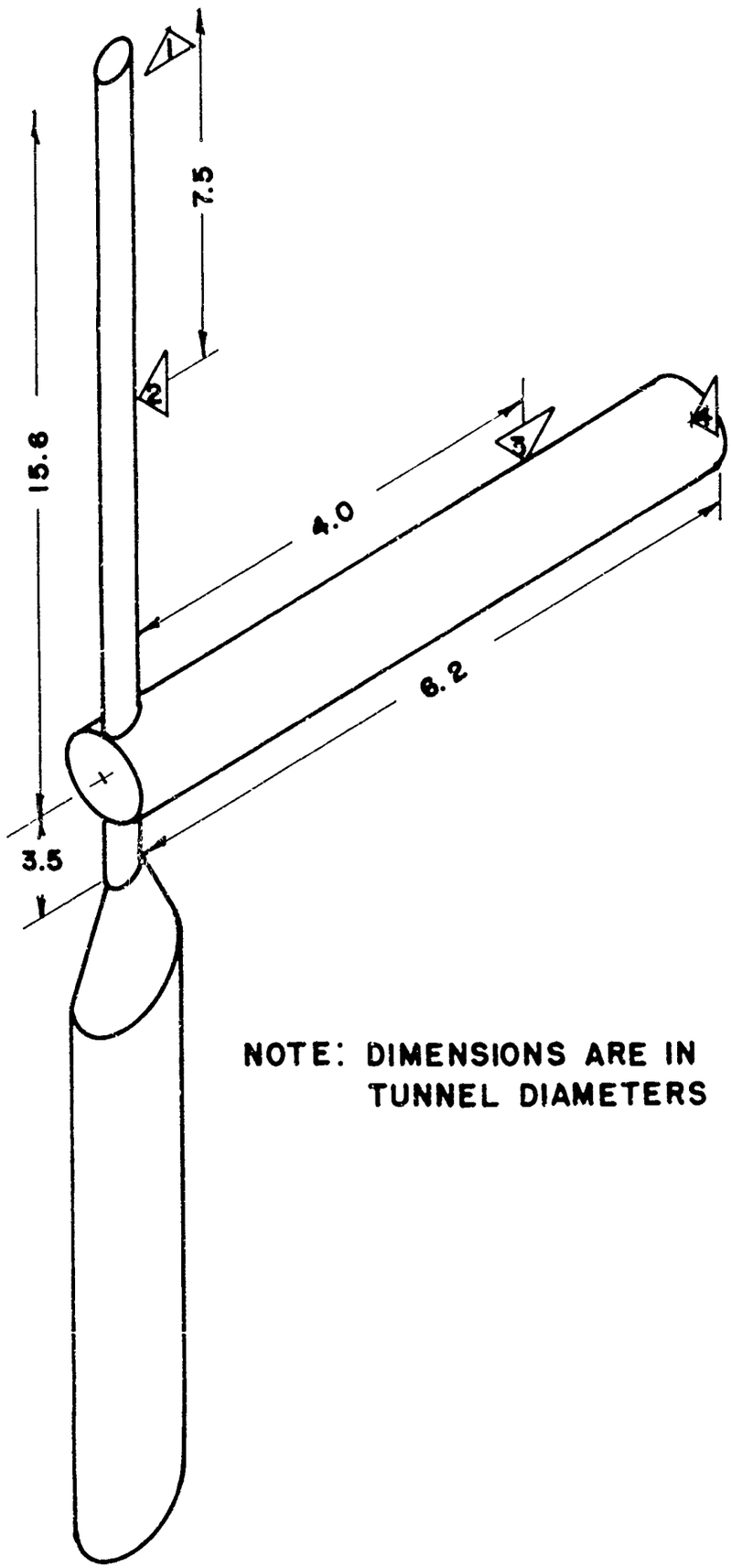

FIG. 3 MODEL # 3

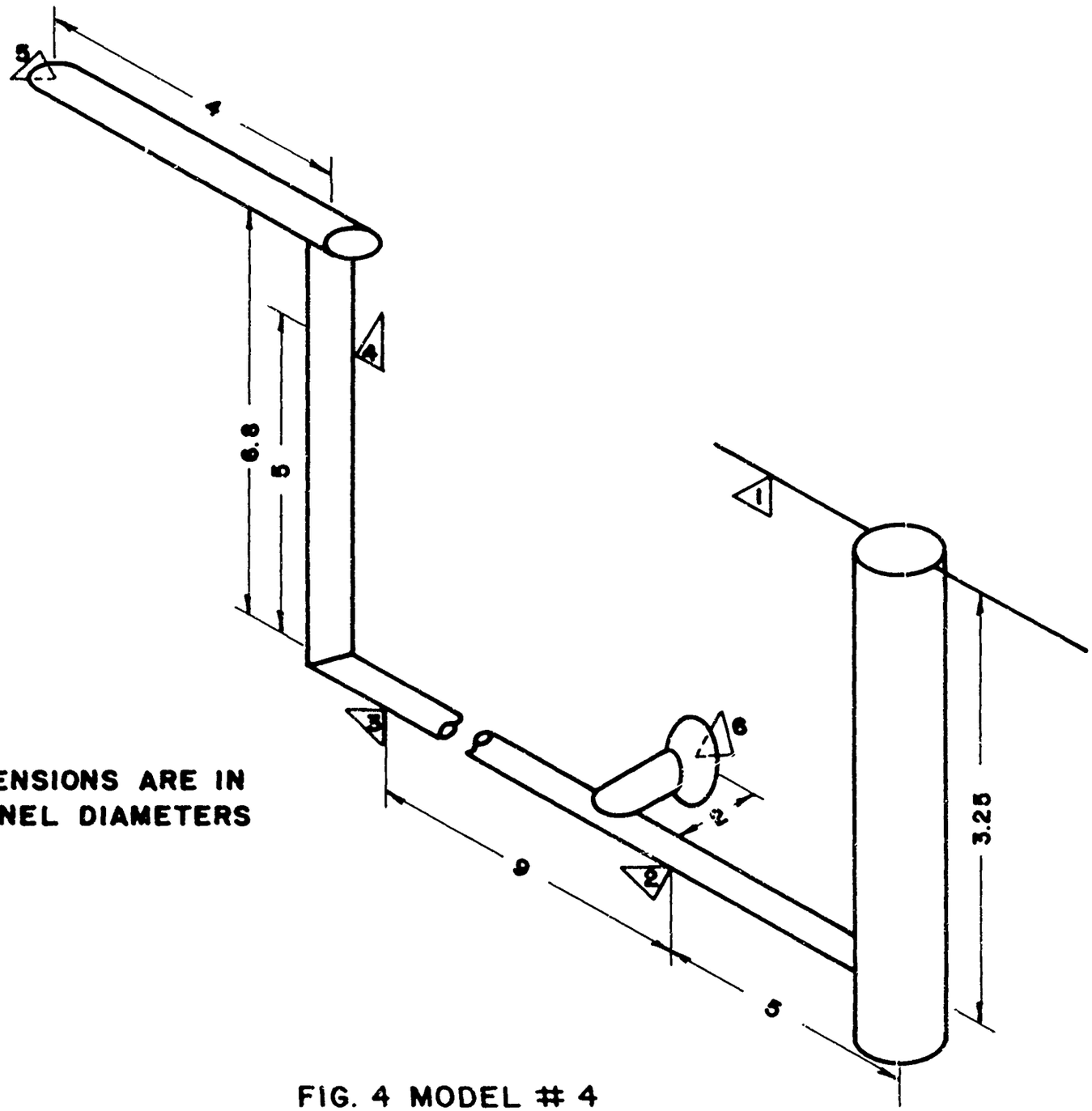

NOTE: DIMENSIONS ARE IN TUNNEL DIAMETERS

FIG. 4 MODEL # 4

FIG. 5 MOVING TEST SECTION

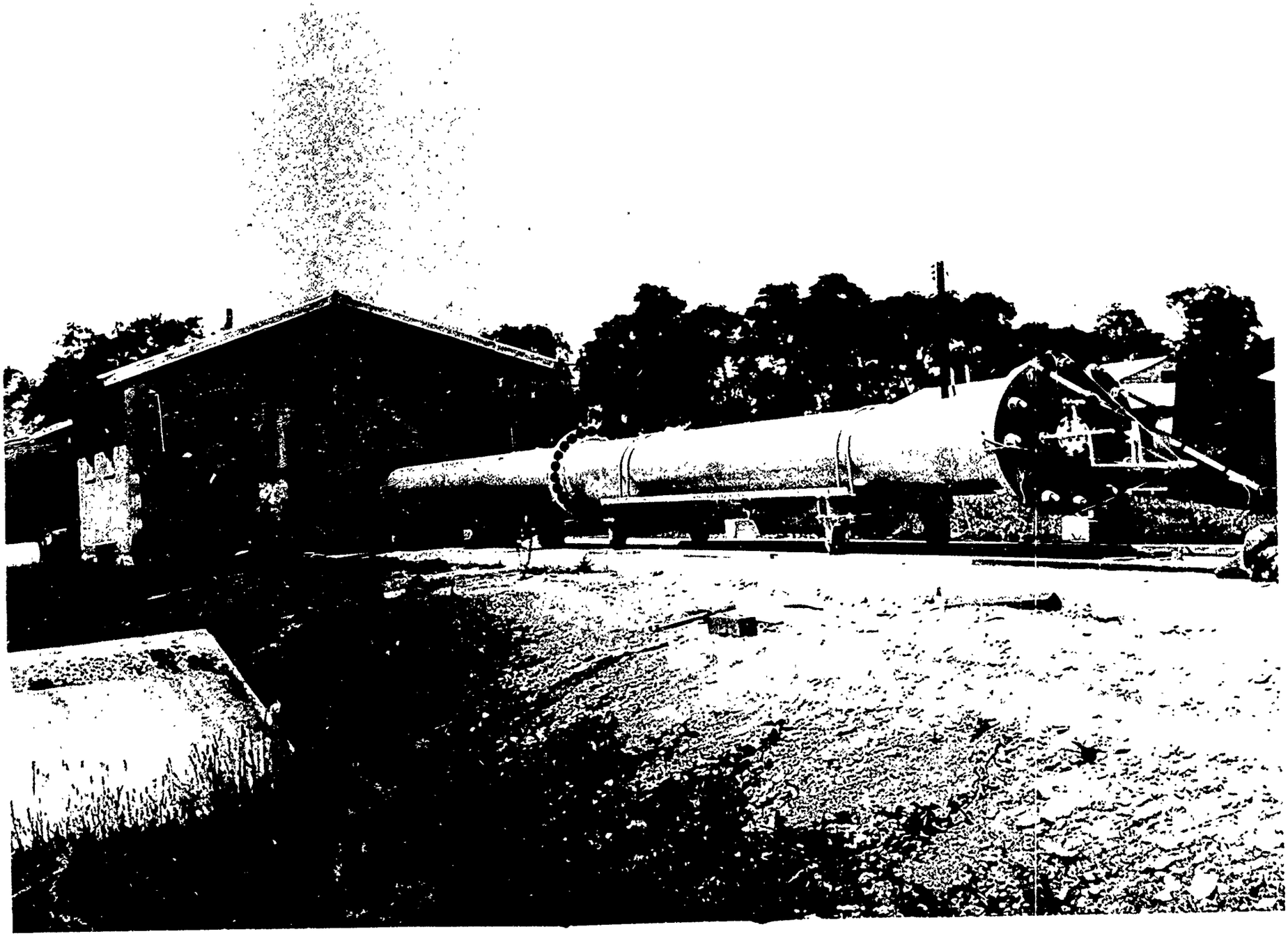

FIG. 6 MODEL ATTACHED TO TEST SECTION

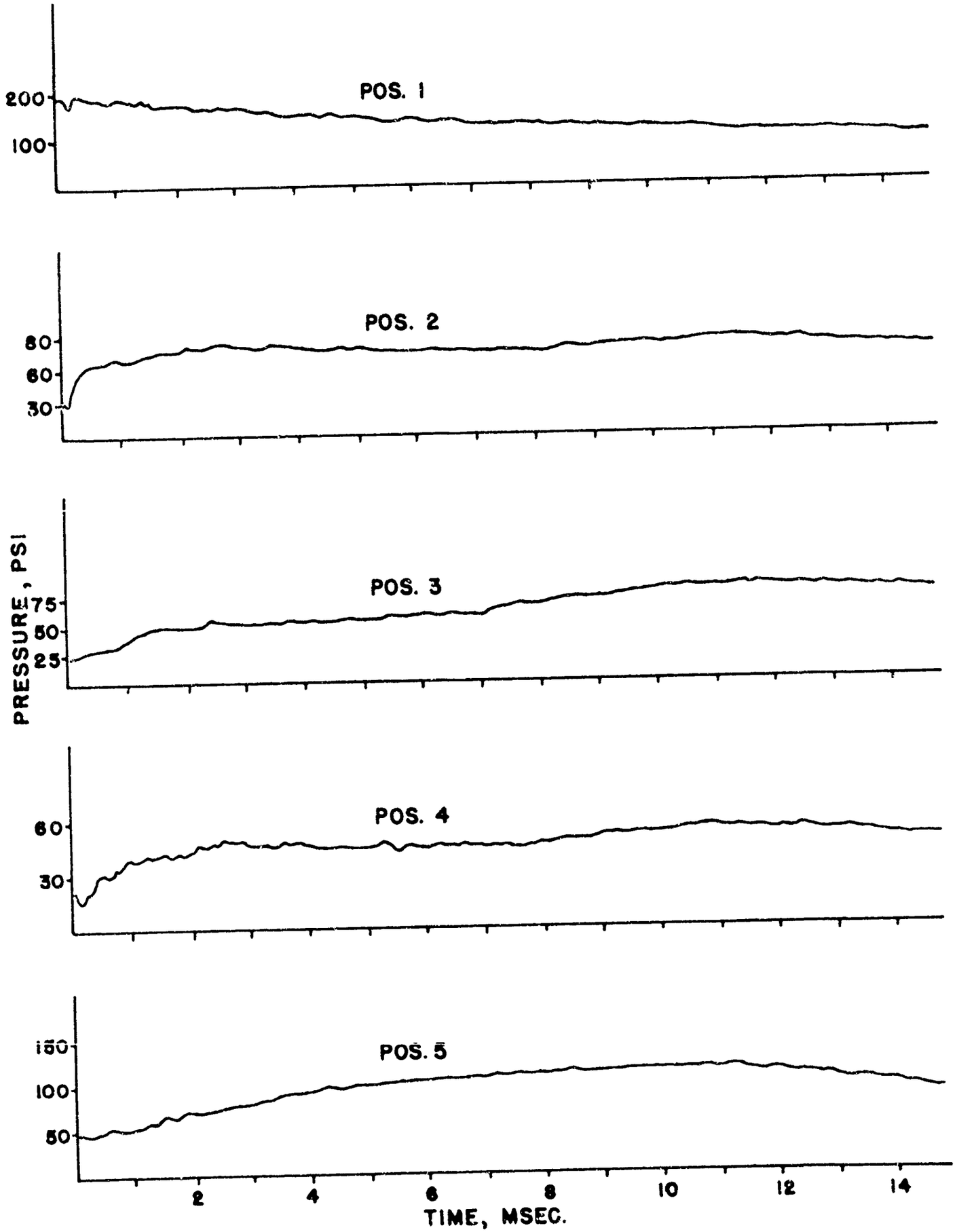

FIG. 7 TYPICAL SHOCK TUBE RECORDS FROM MODEL # 2

FIG. 8 - PRESSURE-TIME PROFILES AT GAGE POSITIONS - MODEL #1

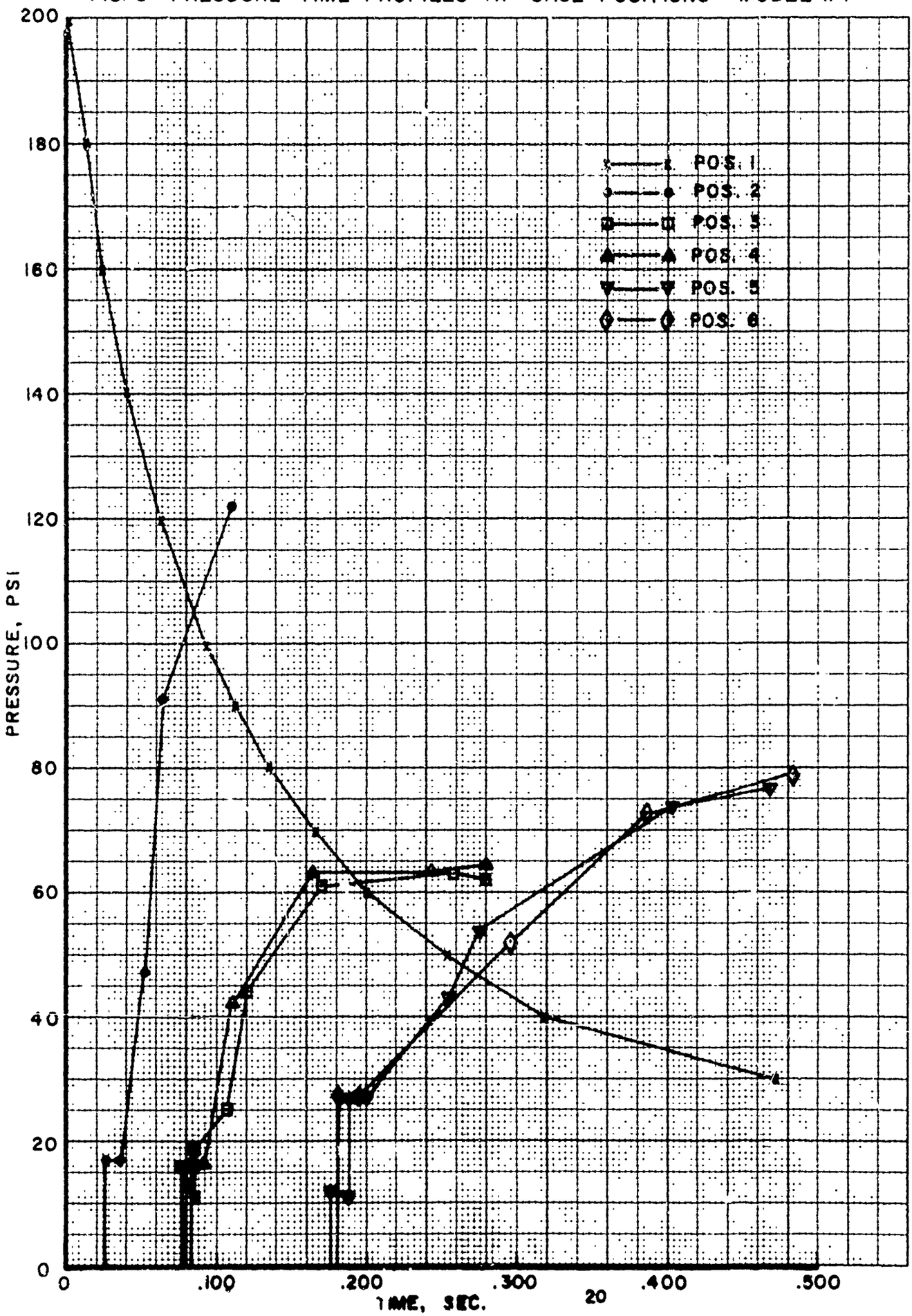

FIG. 9 – PRESSURE-TIME PROFILES AT GAGE POSITIONS – MODEL #1

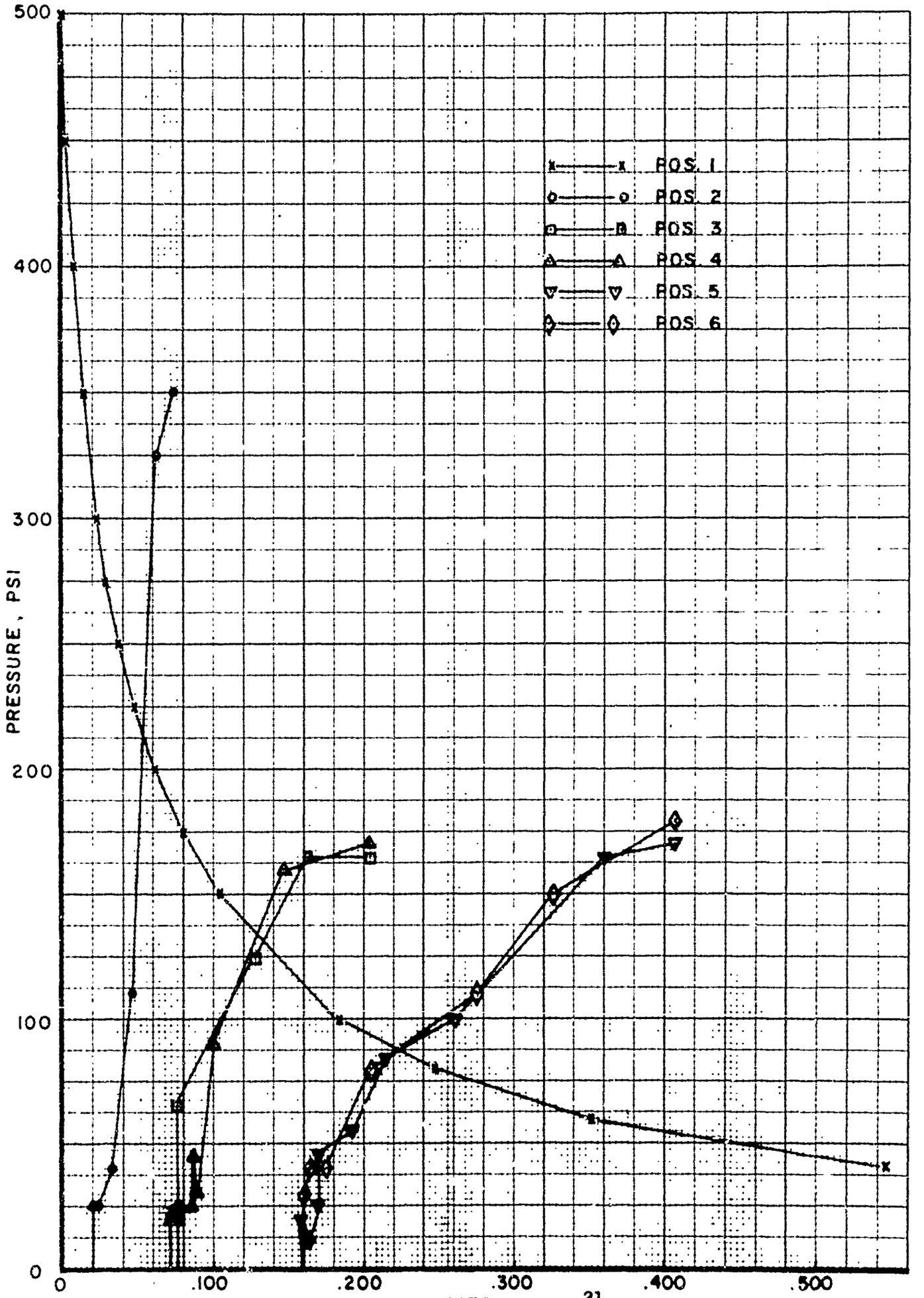

FIG. 10 - PRESSURE-TIME PROFILES AT GAGE POSITIONS - MODEL # 1

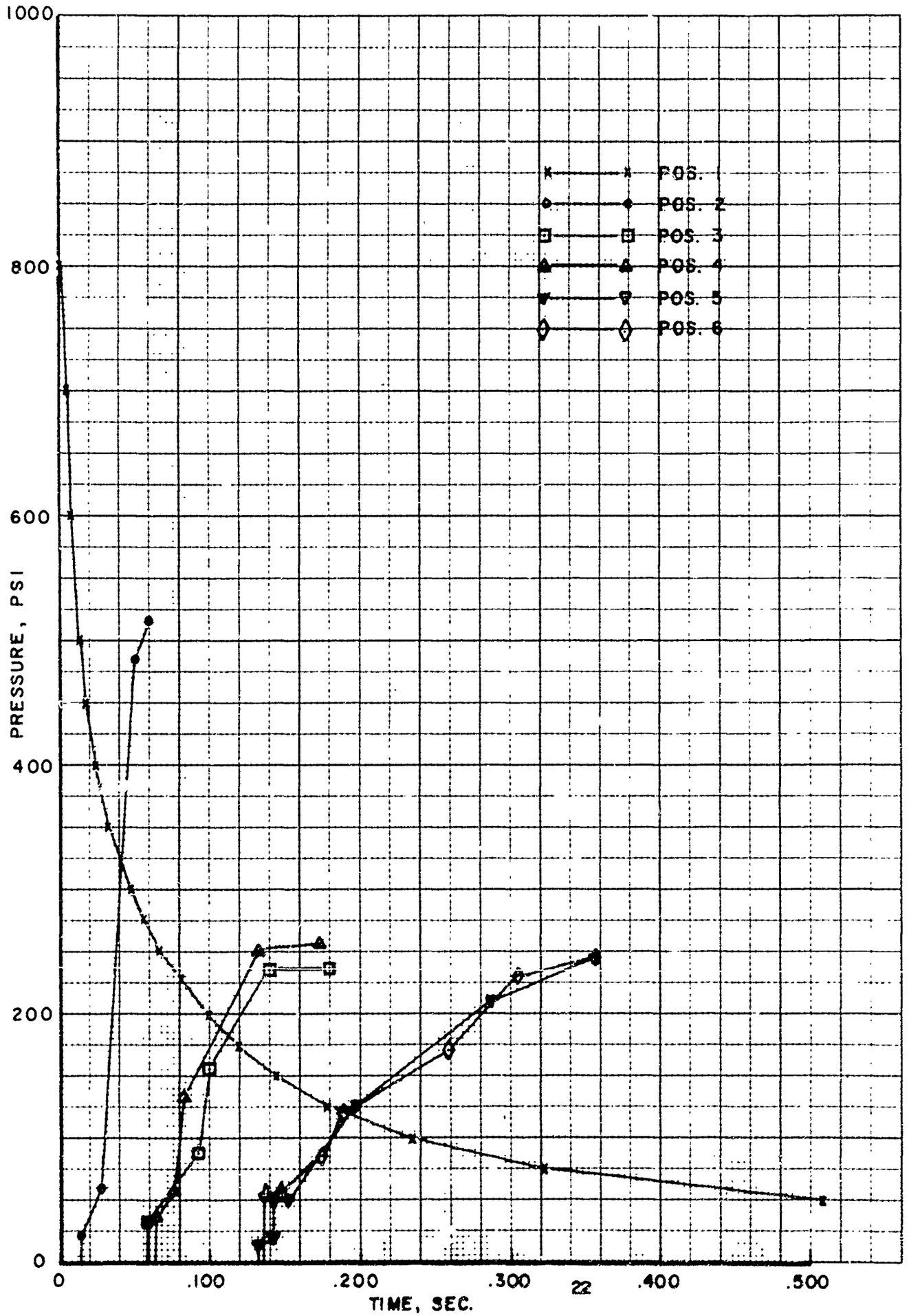

FIG. 11 - PRESSURE-TIME PROFILE AT GAGE POSITIONS - MODEL # 2

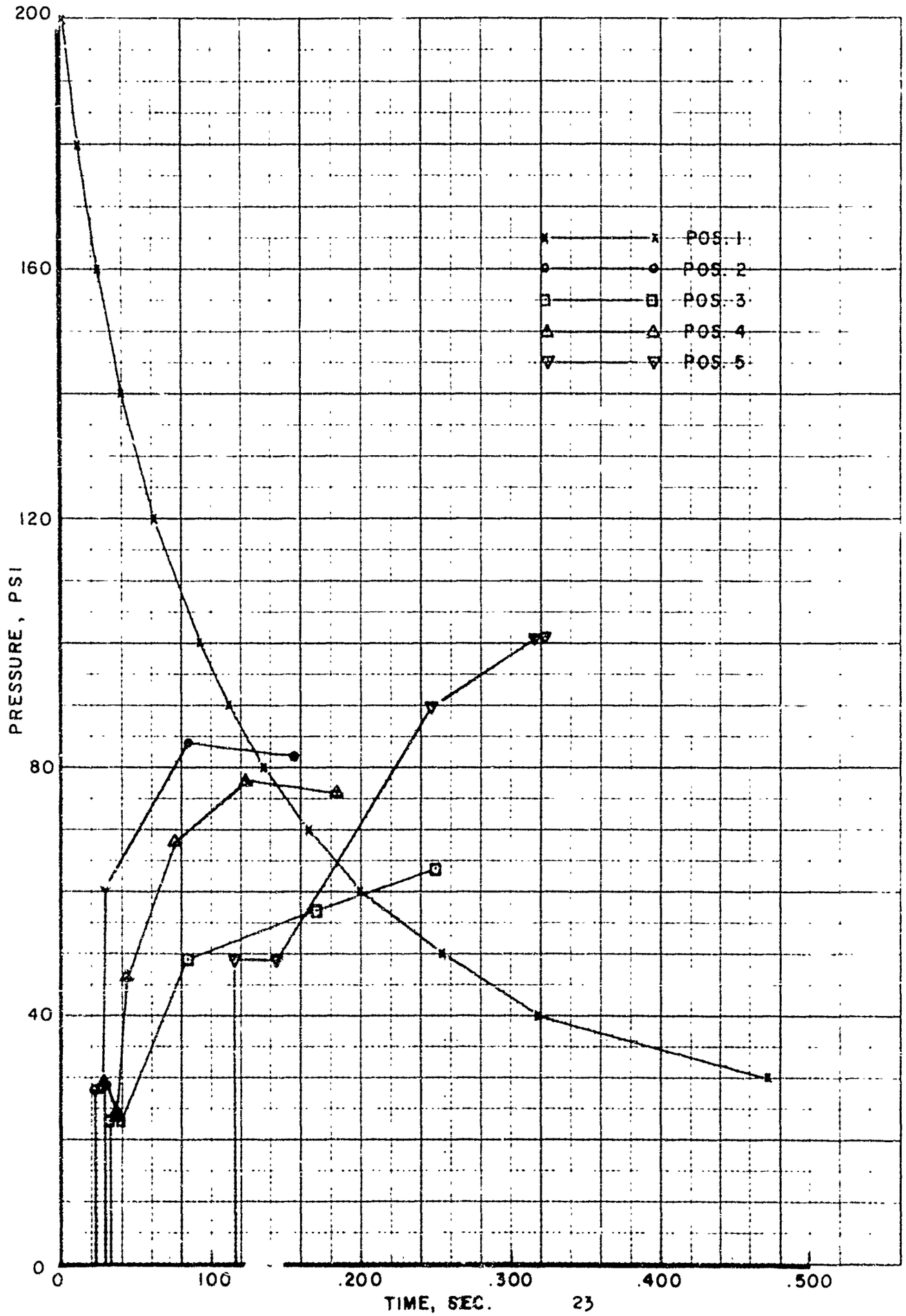

FIG. 12 - PRESSURE-TIME PROFILES AT GAGE POSITIONS - MODEL # 2

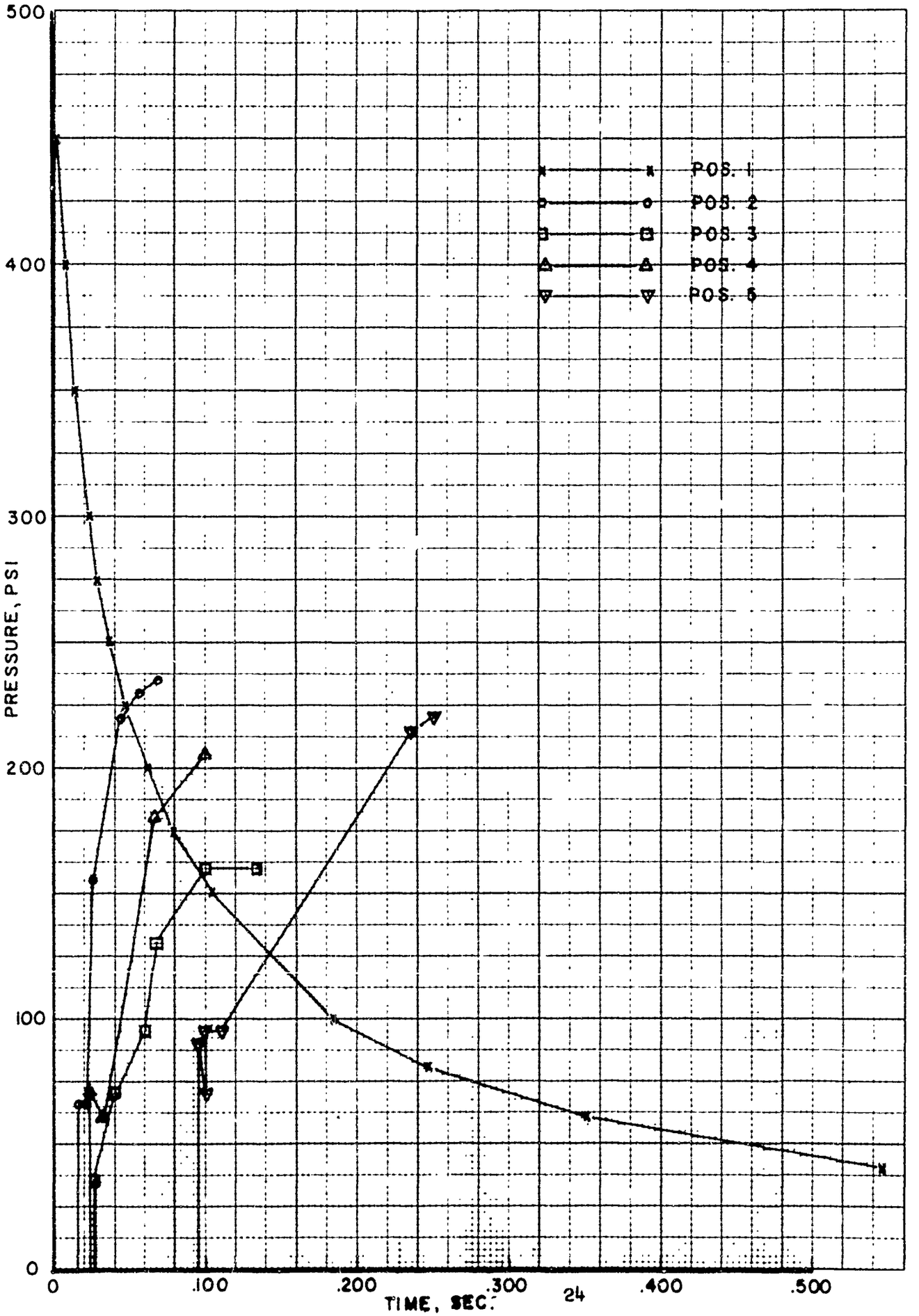

FIG. 13 - PRESSURE-TIME PROFILES AT GAGE POSITIONS - MODEL # 2

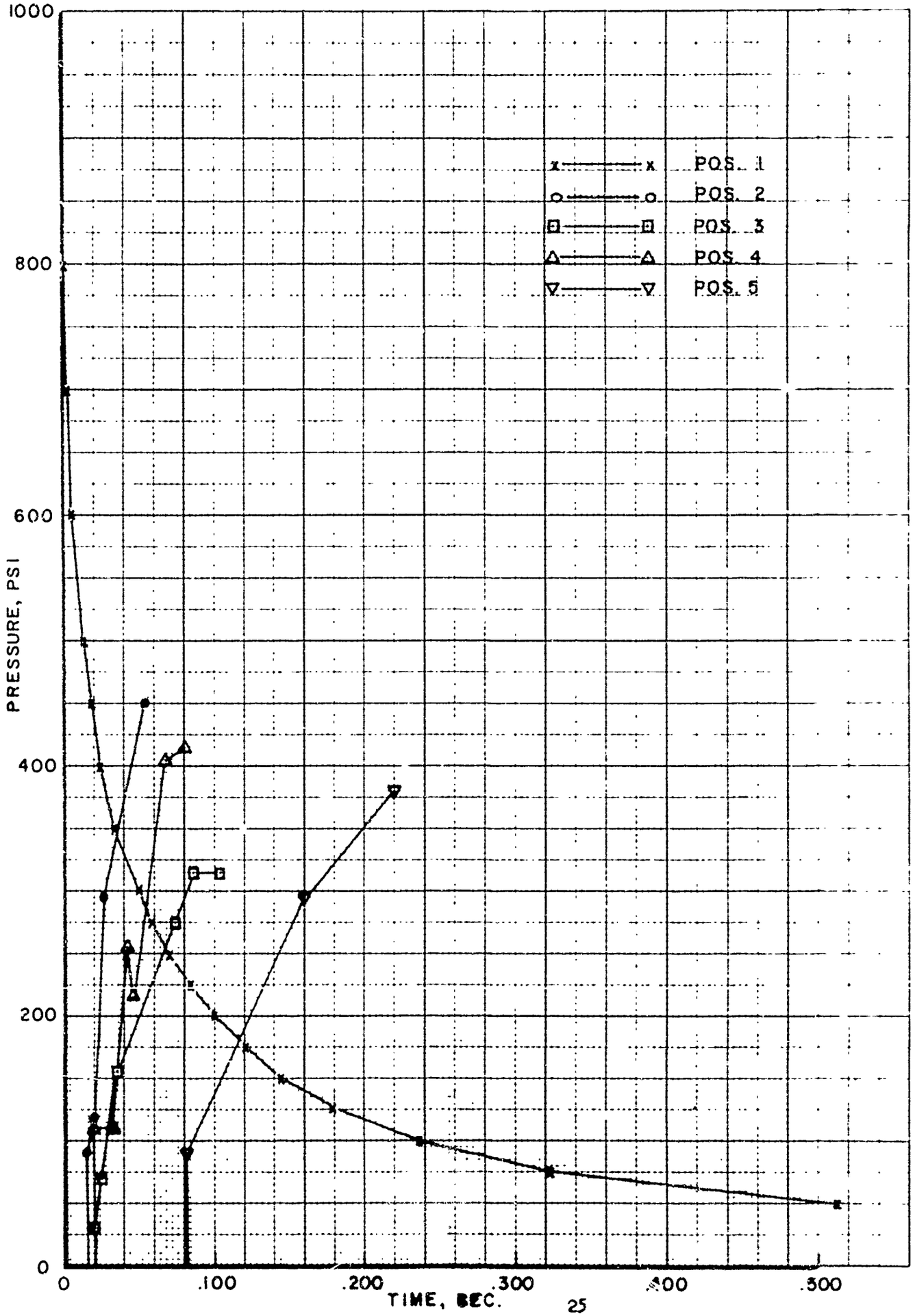

FIG. 14– PRESSURE-TIME PROFILES AT GAGE POSITIONS - MODEL #3

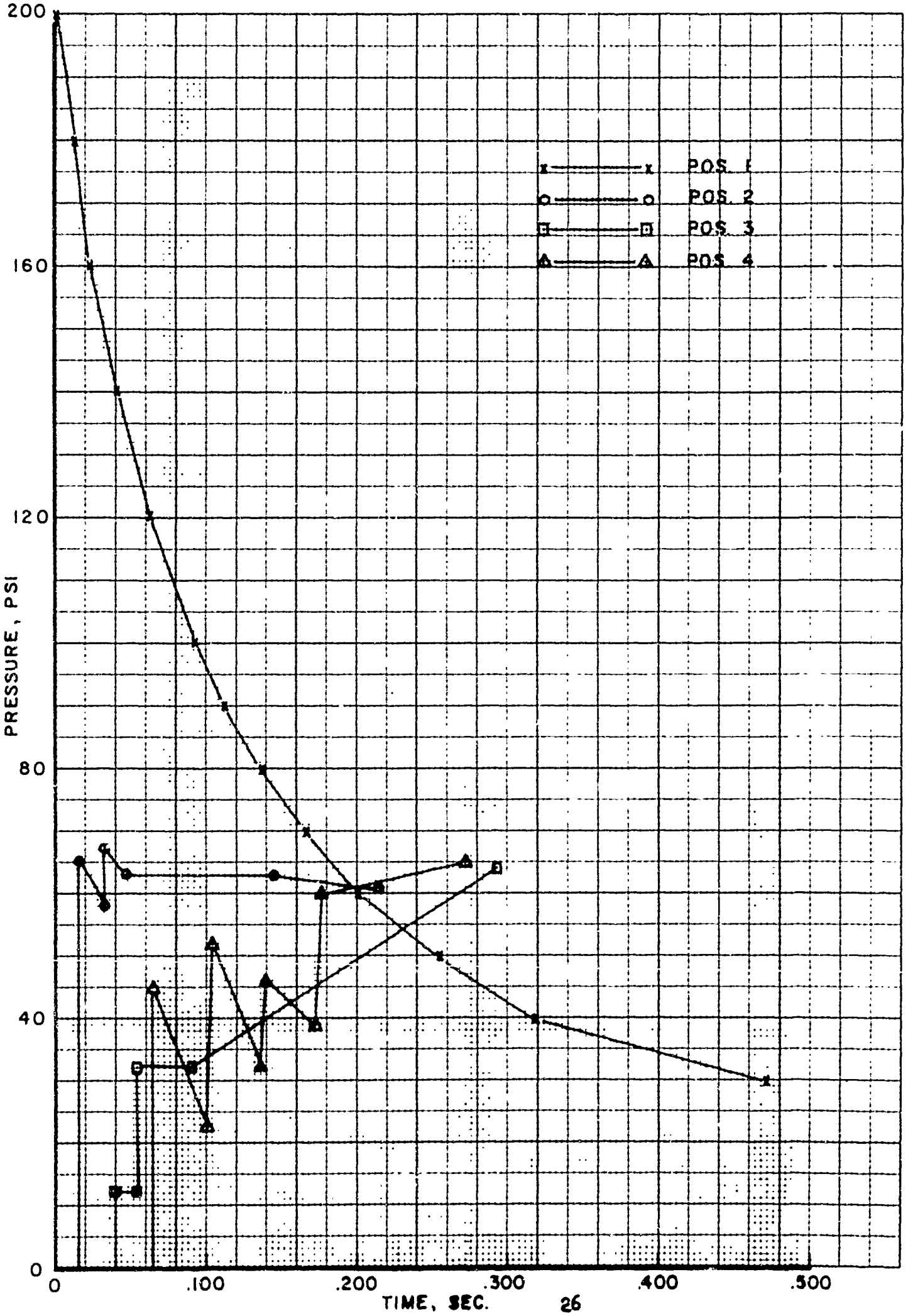

FIG. 15 - PRESSURE-TIME PROFILES AT GAGE POSITIONS - MODEL # 3

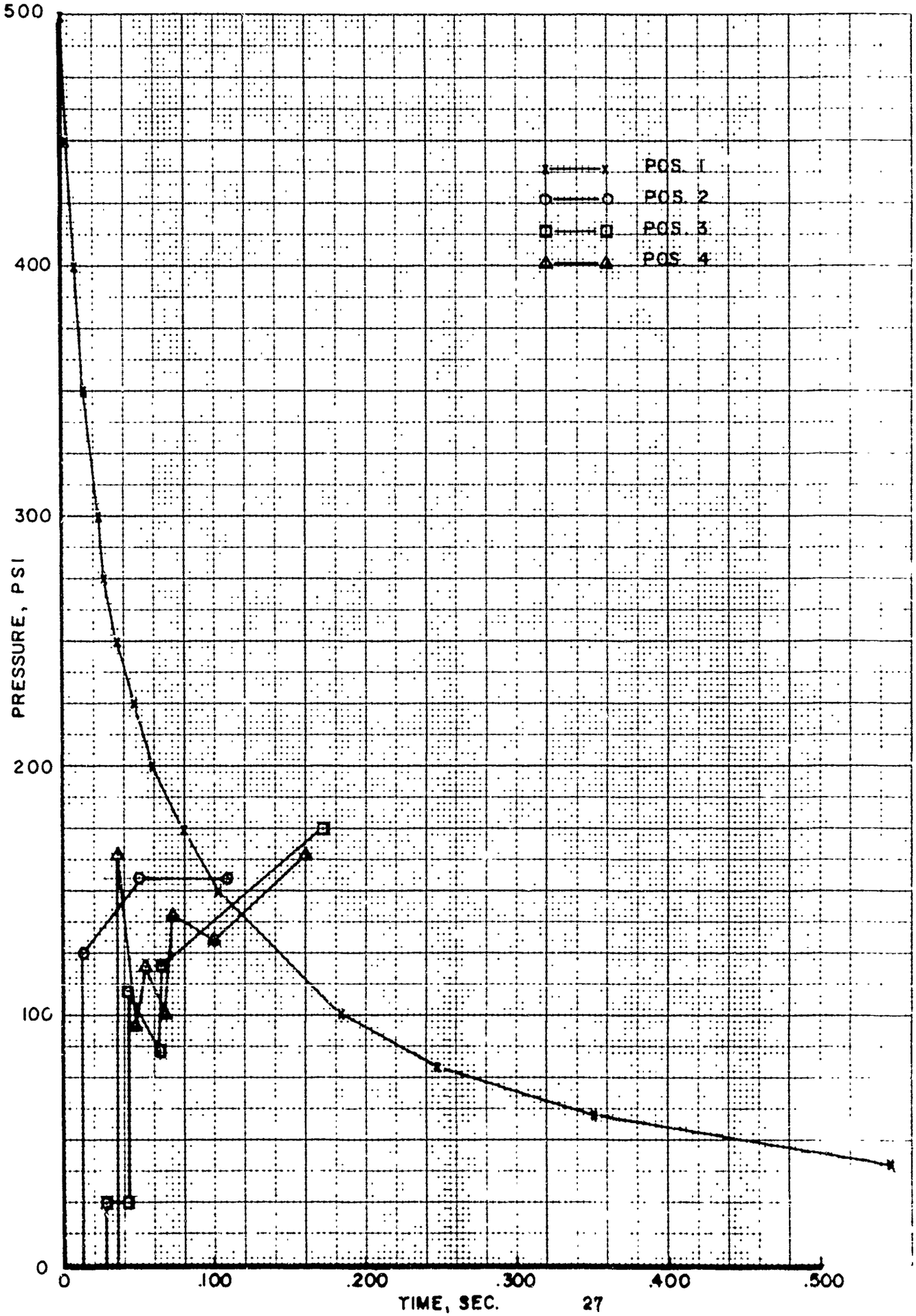

FIG. 16 – PRESSURE-TIME PROFILES AT GAGE POSITIONS – MODEL # 3

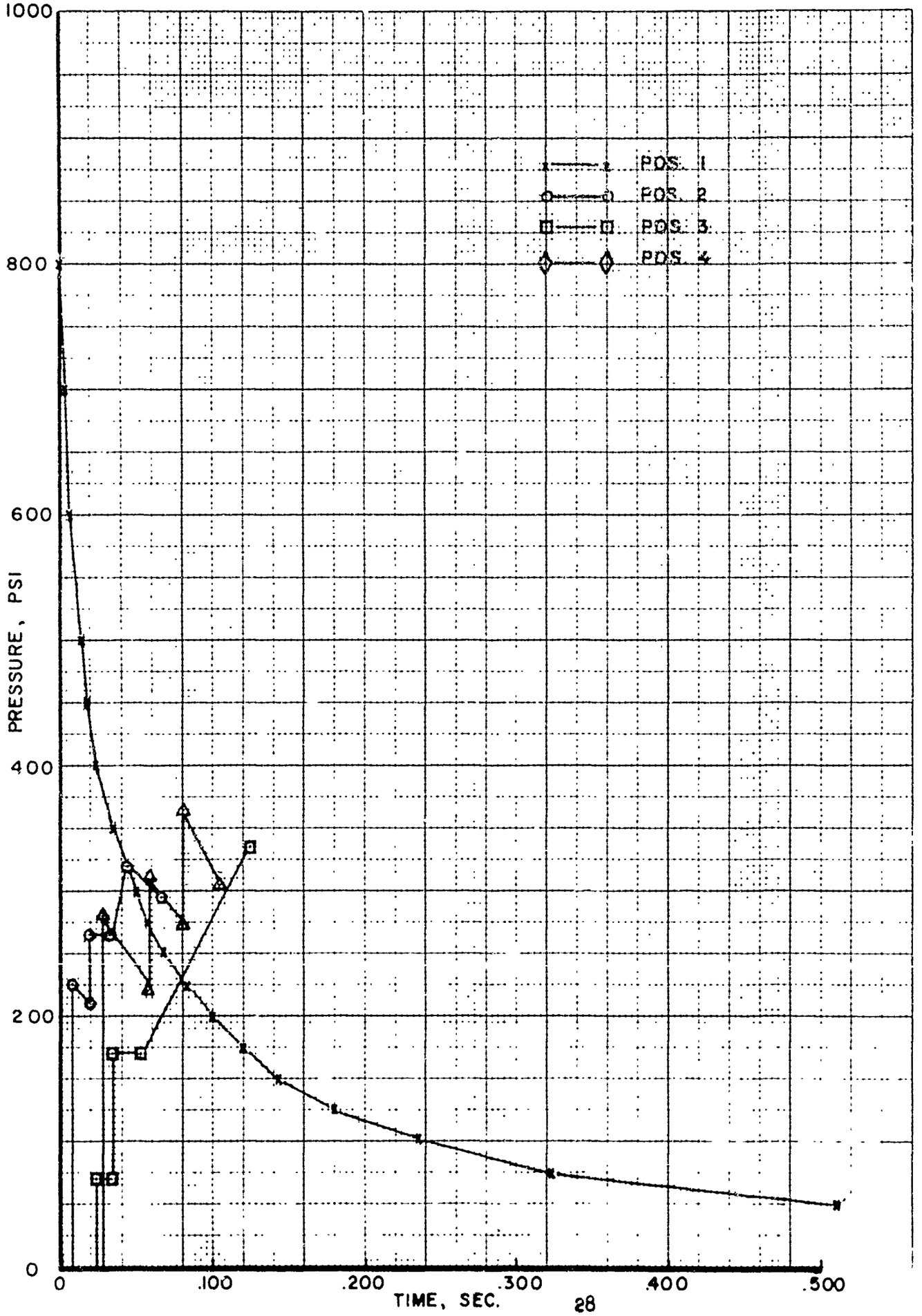

FIG. 17- PRESSURE-TIME PROFILES AT GAGE POSITIONS—MODEL # 4

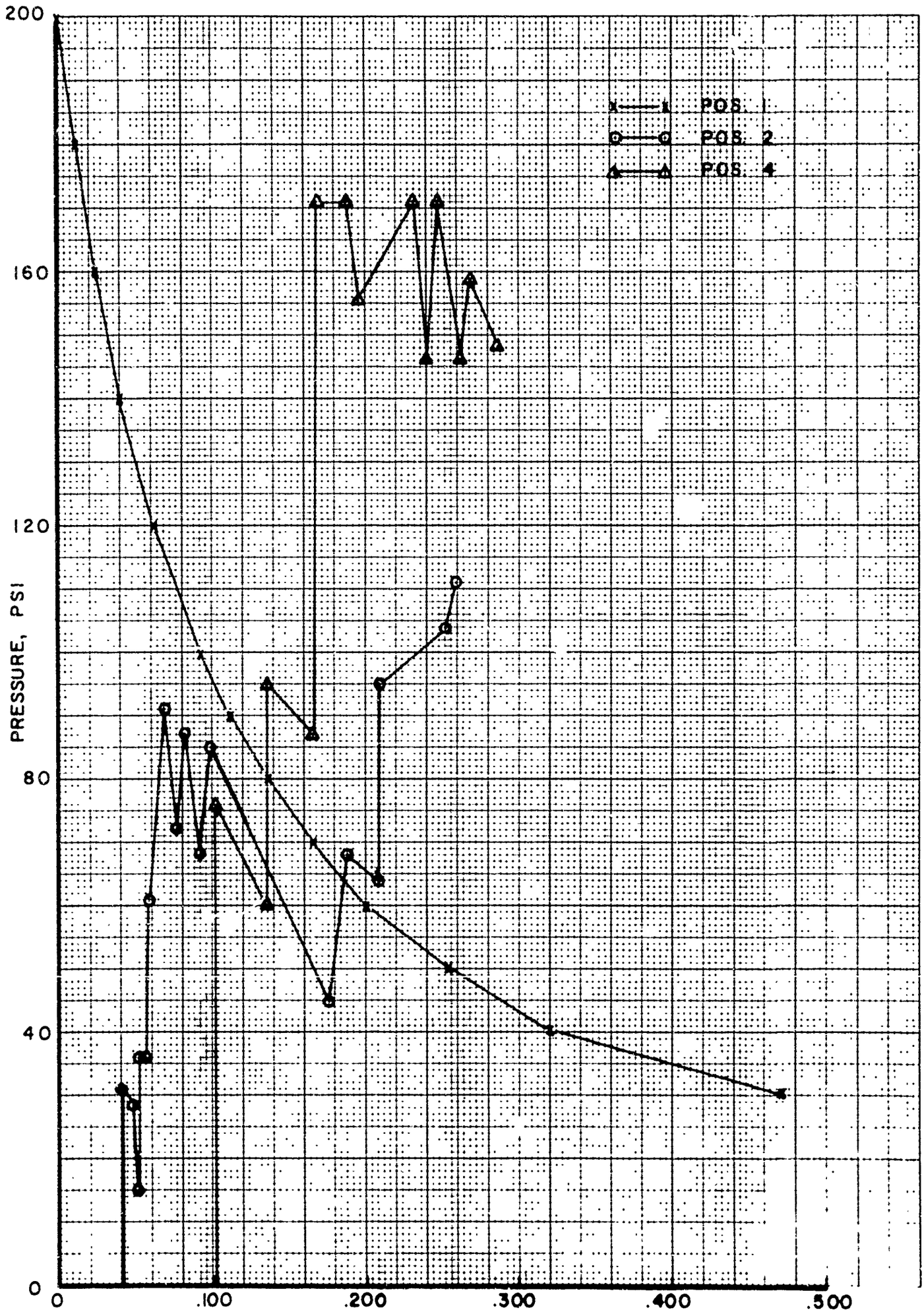

FIG. 18 - PRESSURE-TIME PROFILES AT GAGE POSITIONS - MODEL #4

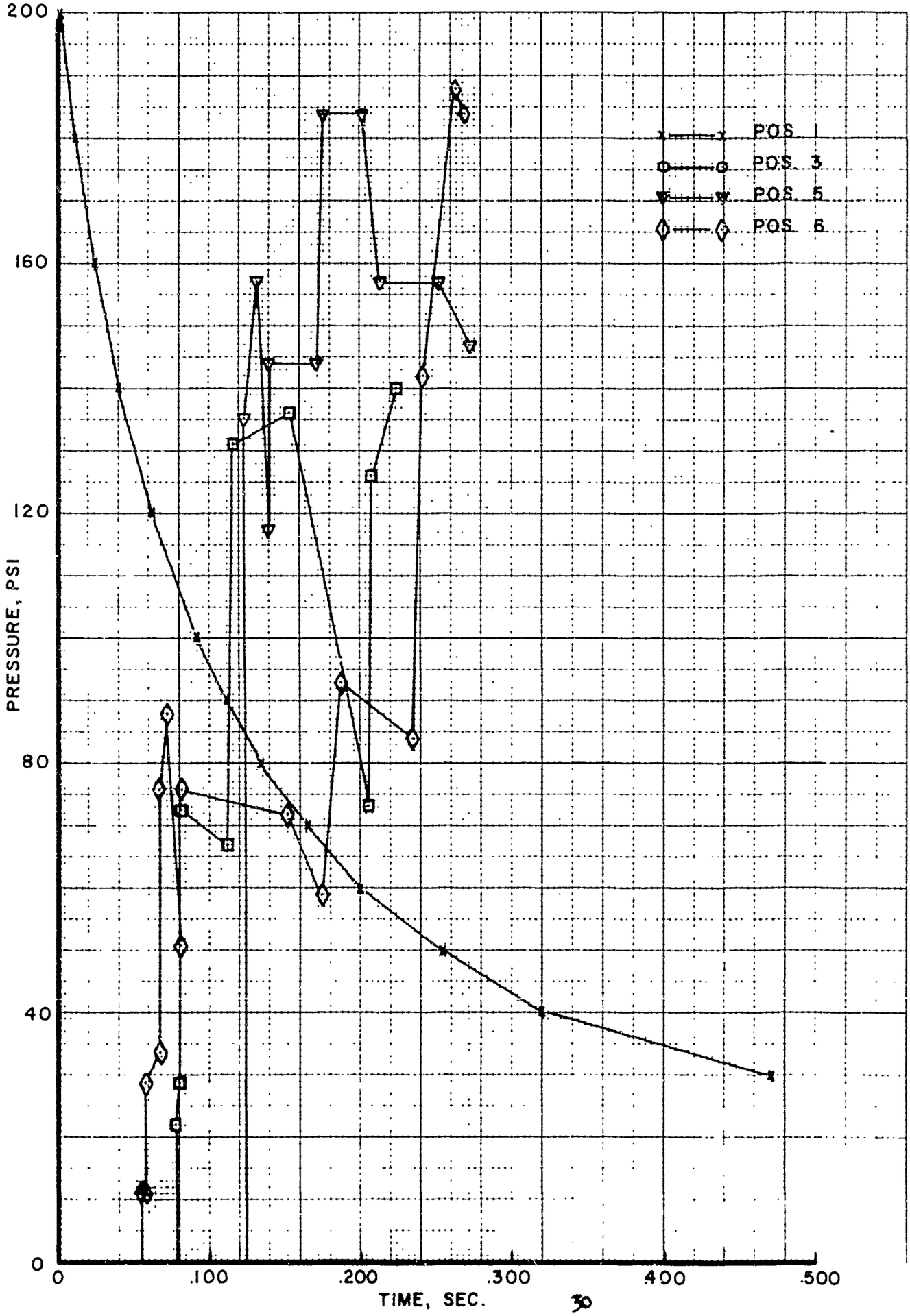

FIG. 19 - PRESSURE-TIME PROFILES AT GAGE POSITIONS - MODEL #4

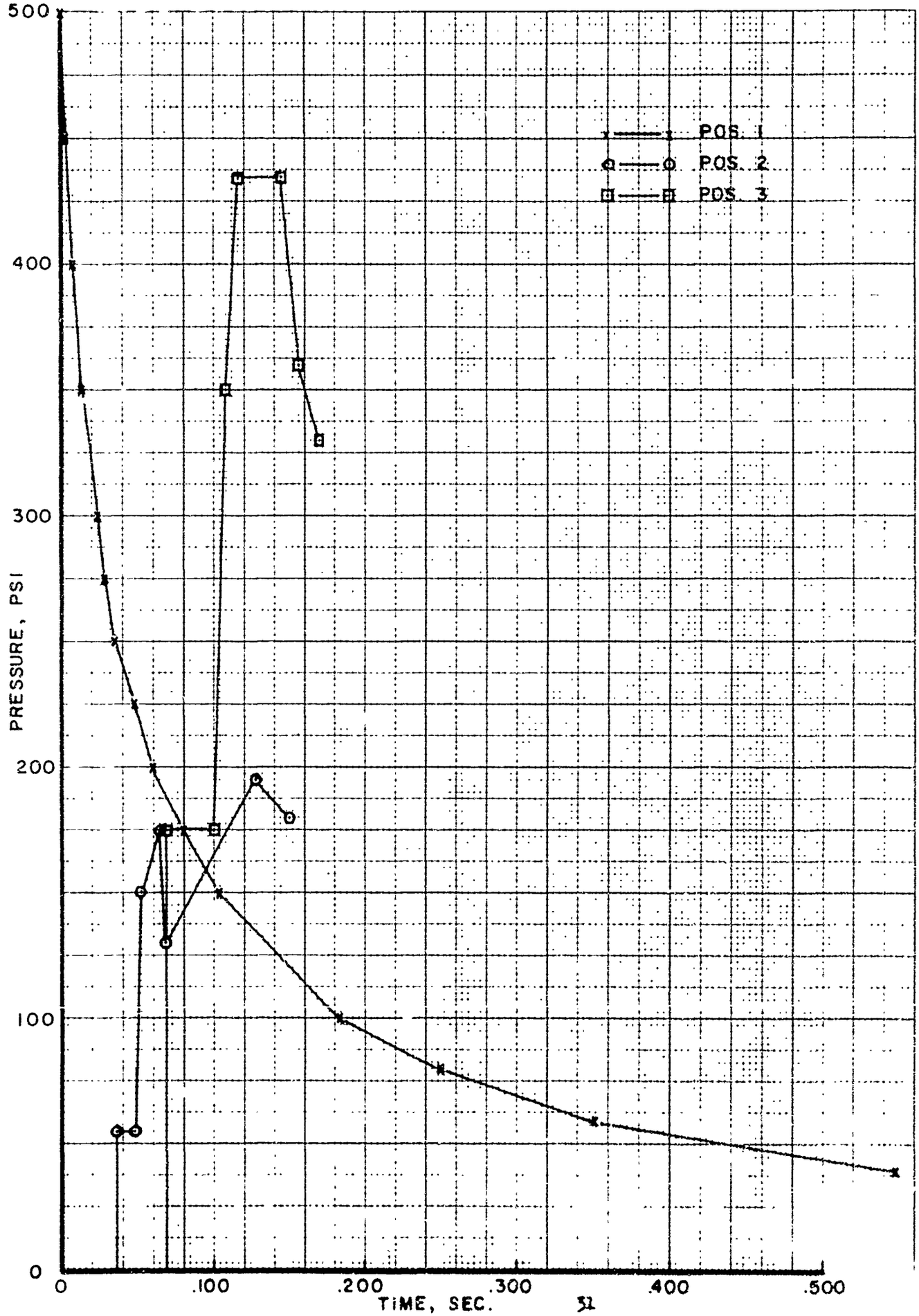

FIG. 20 - PRESSURE-TIME PROFILES AT GAGE POSITIONS - MODEL # 4

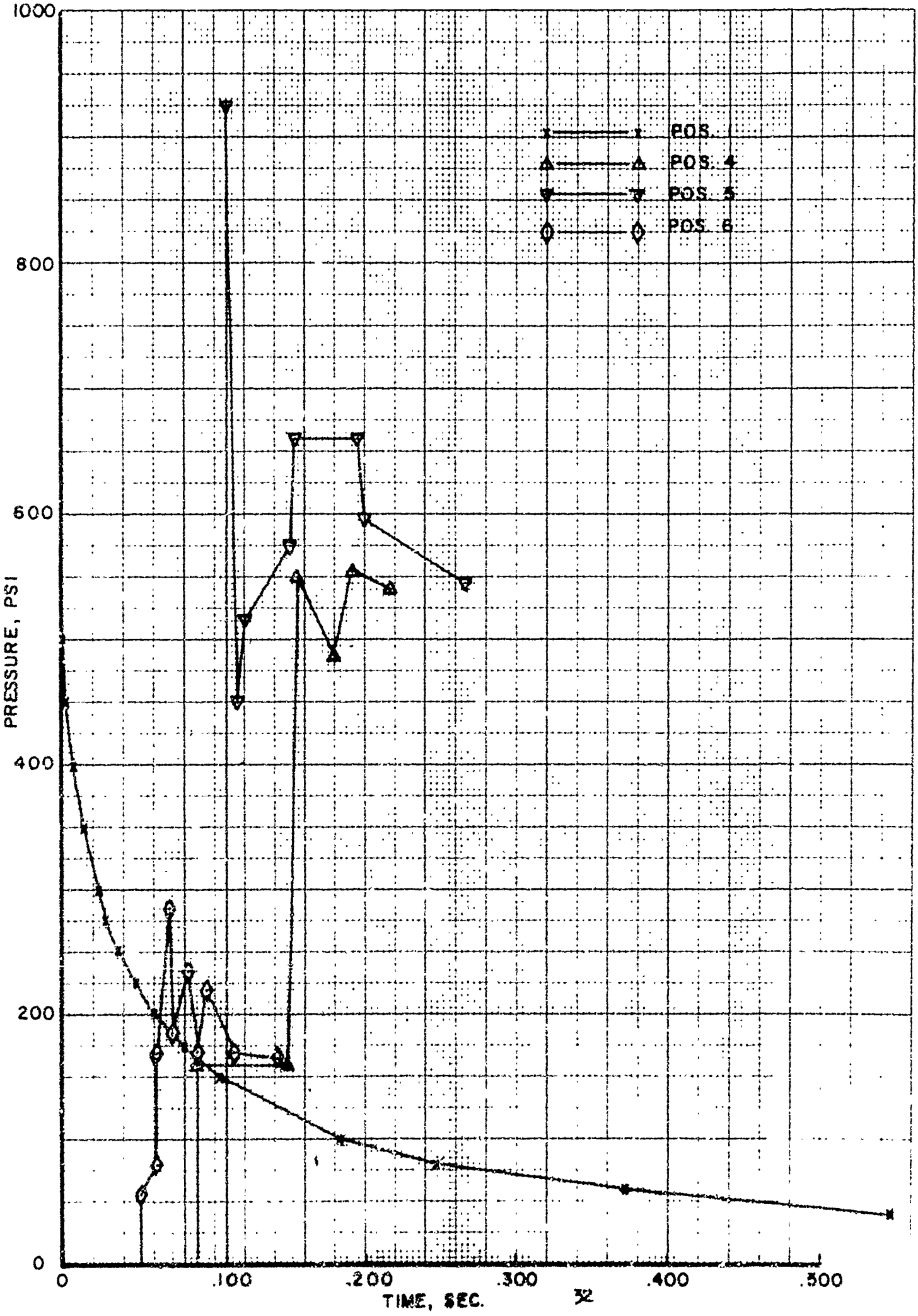

FIG. 21 - PRESSURE-TIME PROFILES AT GAGE POSITIONS - MODEL #4

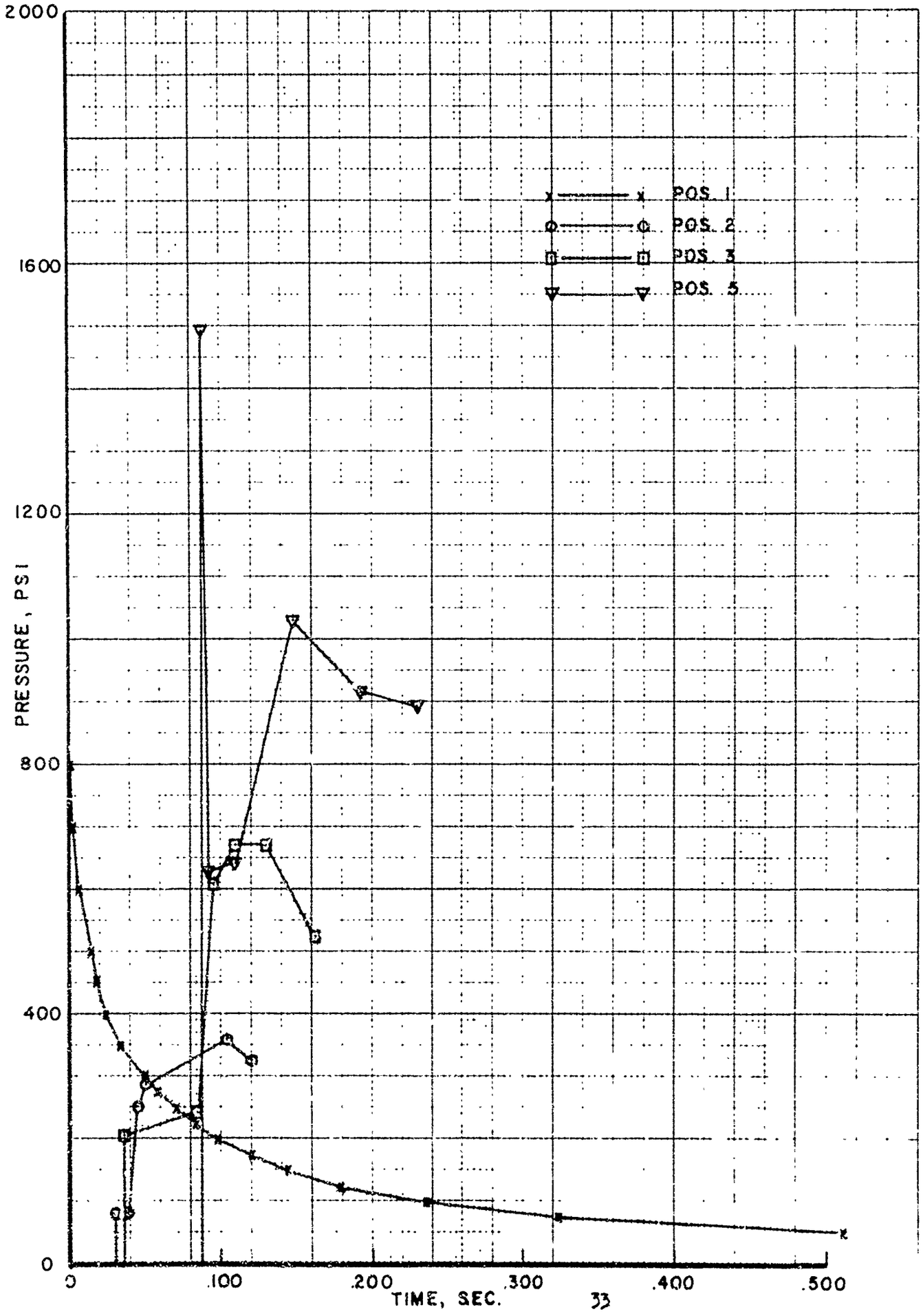

FIG. 22- PRESSURE-TIME PROFILES AT GAGE POSITIONS - MODEL # 4

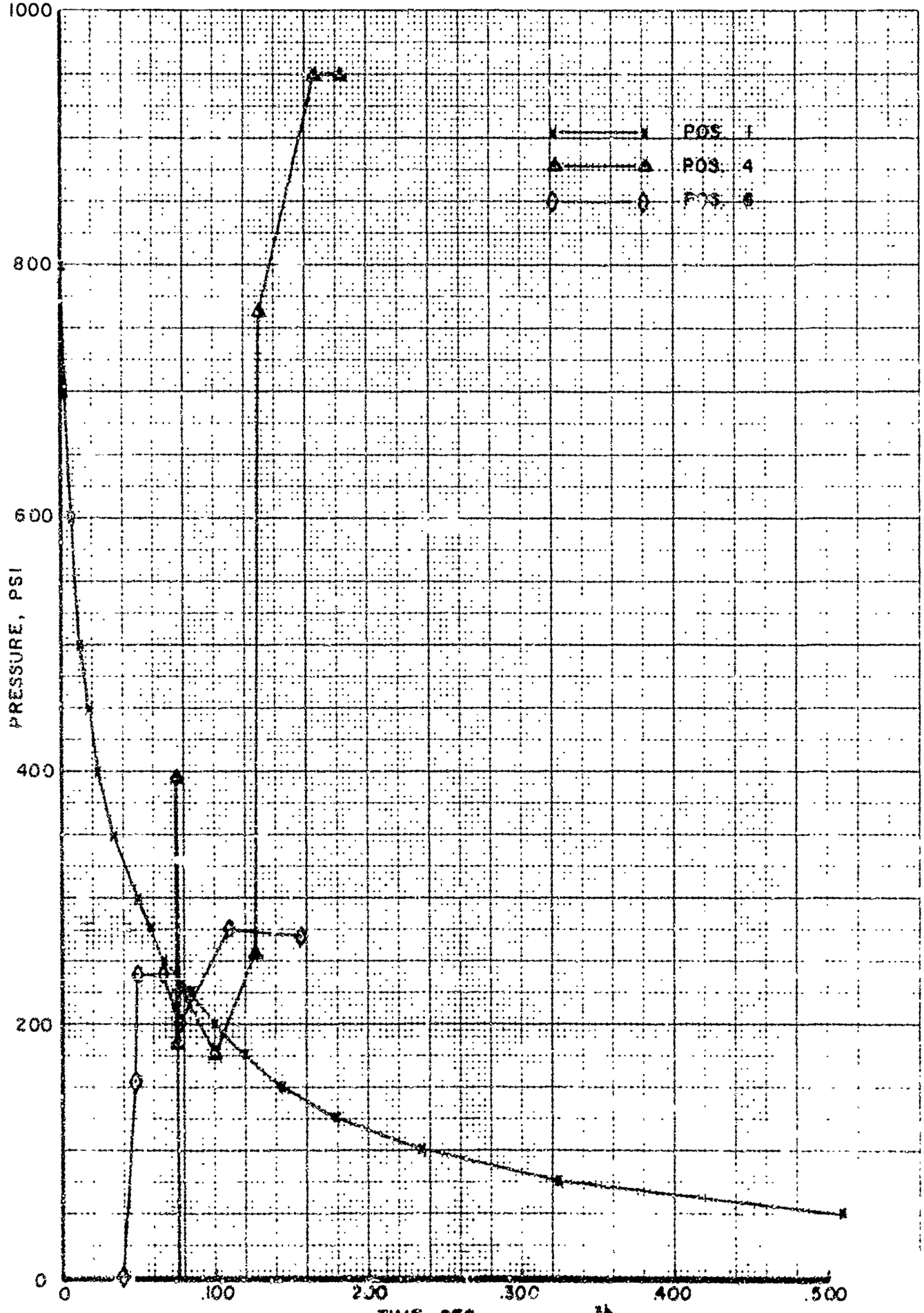

FIG. 23 - INCIDENT SHOCK OVERPRESSURE vs. INITIAL TRANSMITTED SHOCK OVERPRESSURE AT GAGE POSITIONS - MODEL # 1

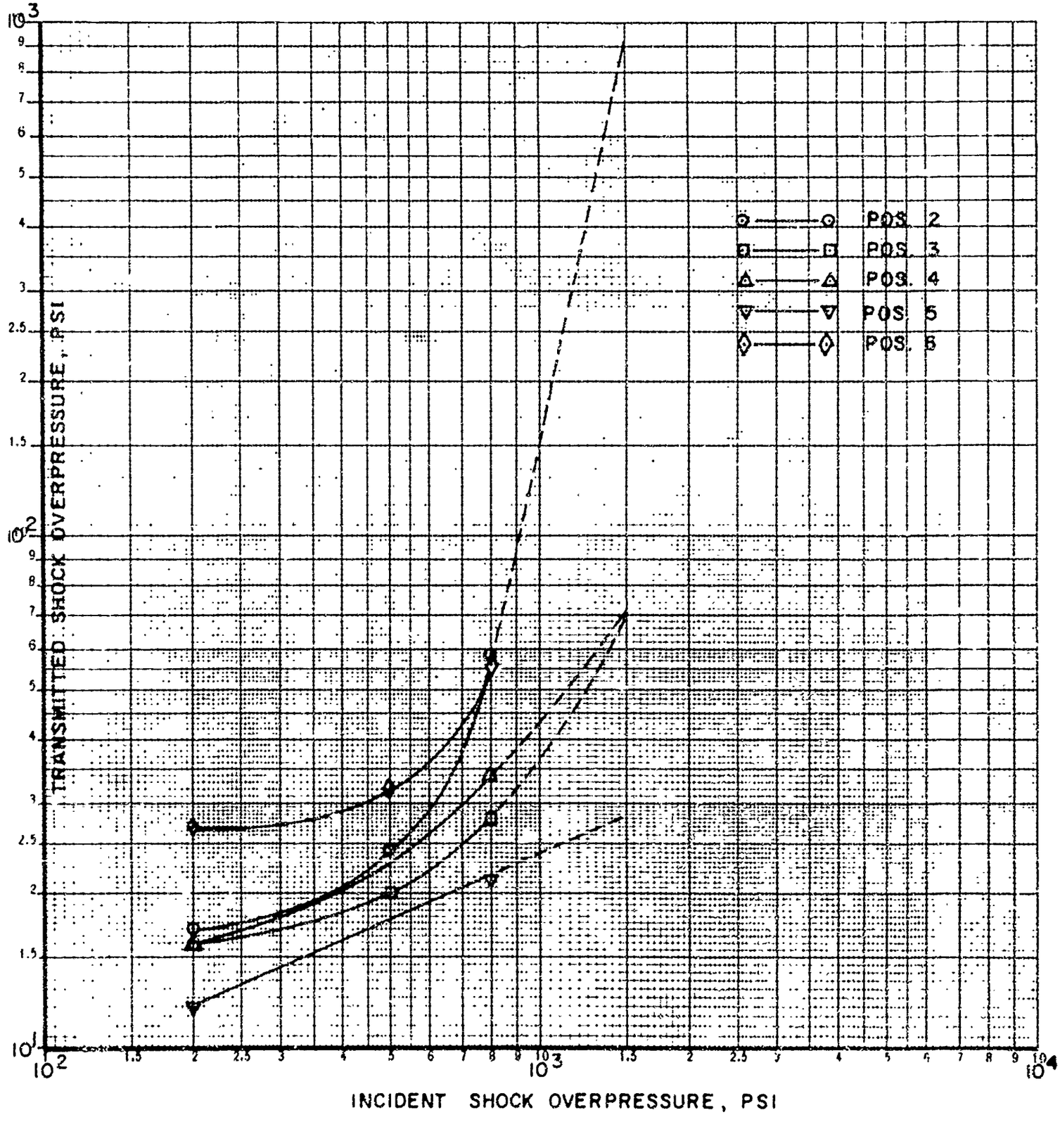

FIG. 24 – INCIDENT SHOCK OVERPRESSURE vs. INITIAL TRANSMITTED SHOCK OVERPRESSURE AT GAGE POSITIONS – MODEL # 2

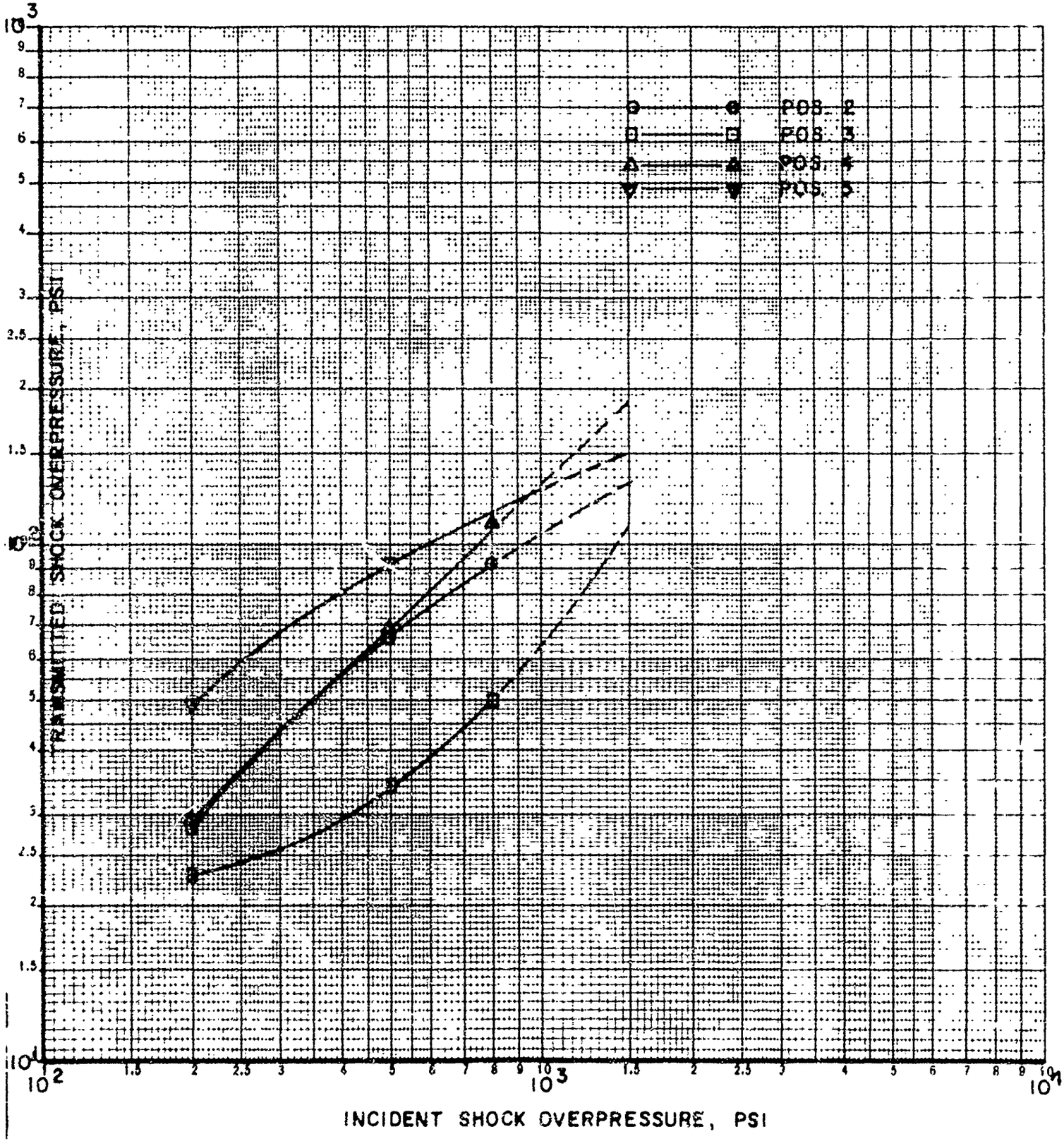

FIG. 25 – INCIDENT SHOCK OVERPRESSURE vs. INITIAL TRANSMITTED SHOCK OVERPRESSURE AT GAGE POSITIONS – MODEL # 3

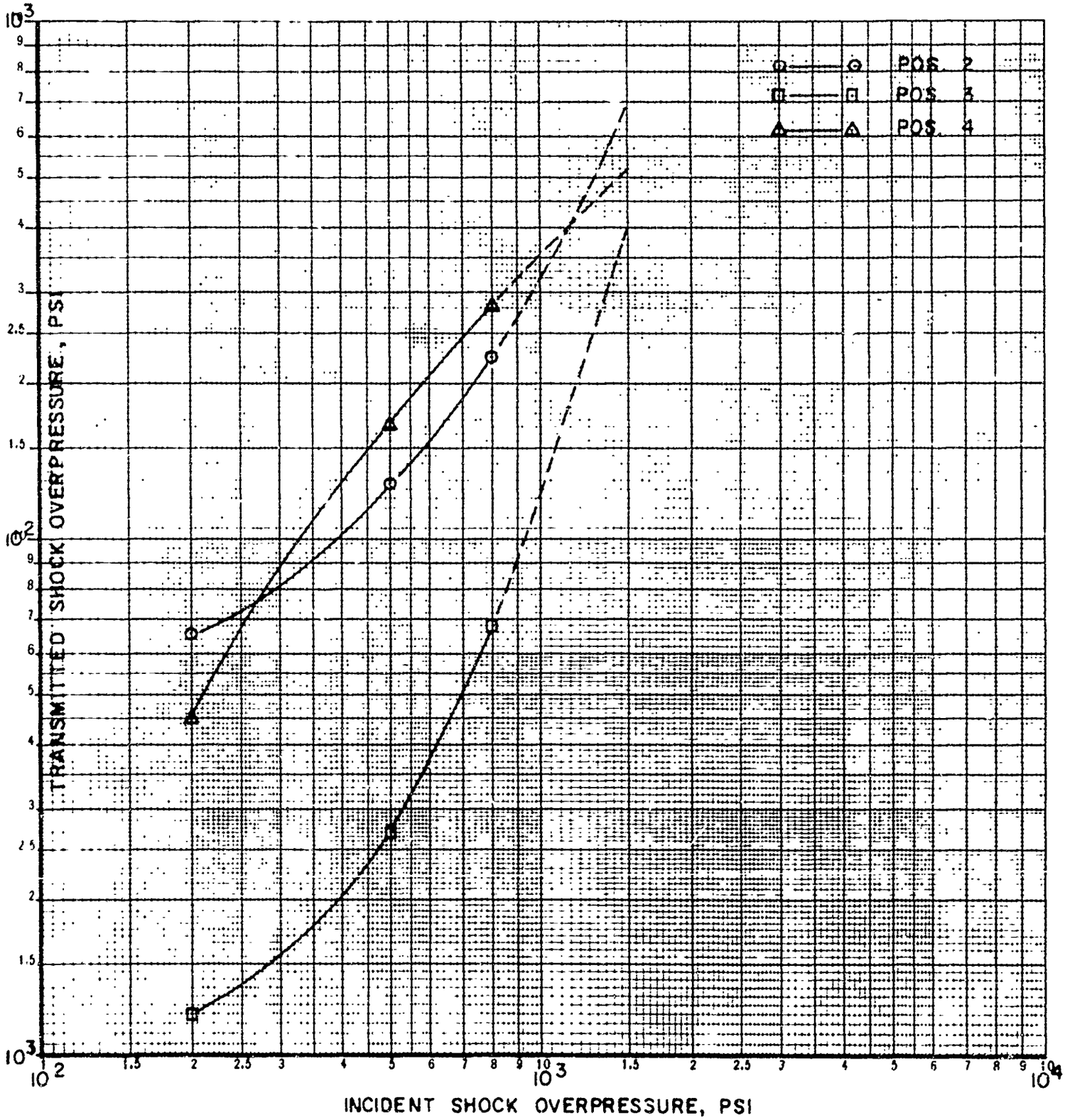

FIG. 26- INCIDENT SHOCK OVERPRESSURE vs. INITIAL TRANSMITTED SHOCK OVERPRESSURE AT GAGE POSITIONS. MODEL #4

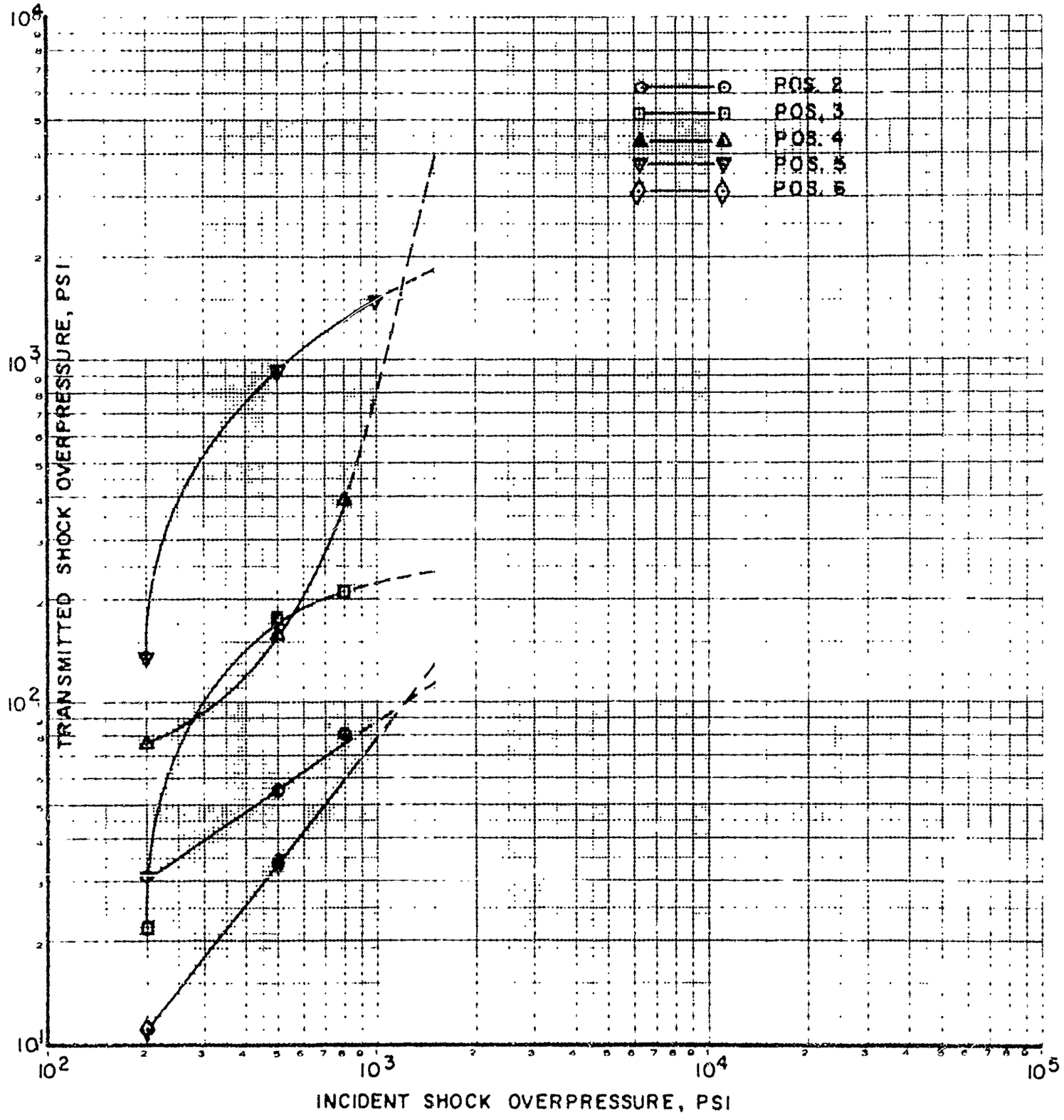

FIG. 27– INCIDENT SHOCK OVERPRESSURE vs. TIME OF ARRIVAL OF TRANSMITTED SHOCK WAVE AT GAGE POSITIONS. MODEL #1.

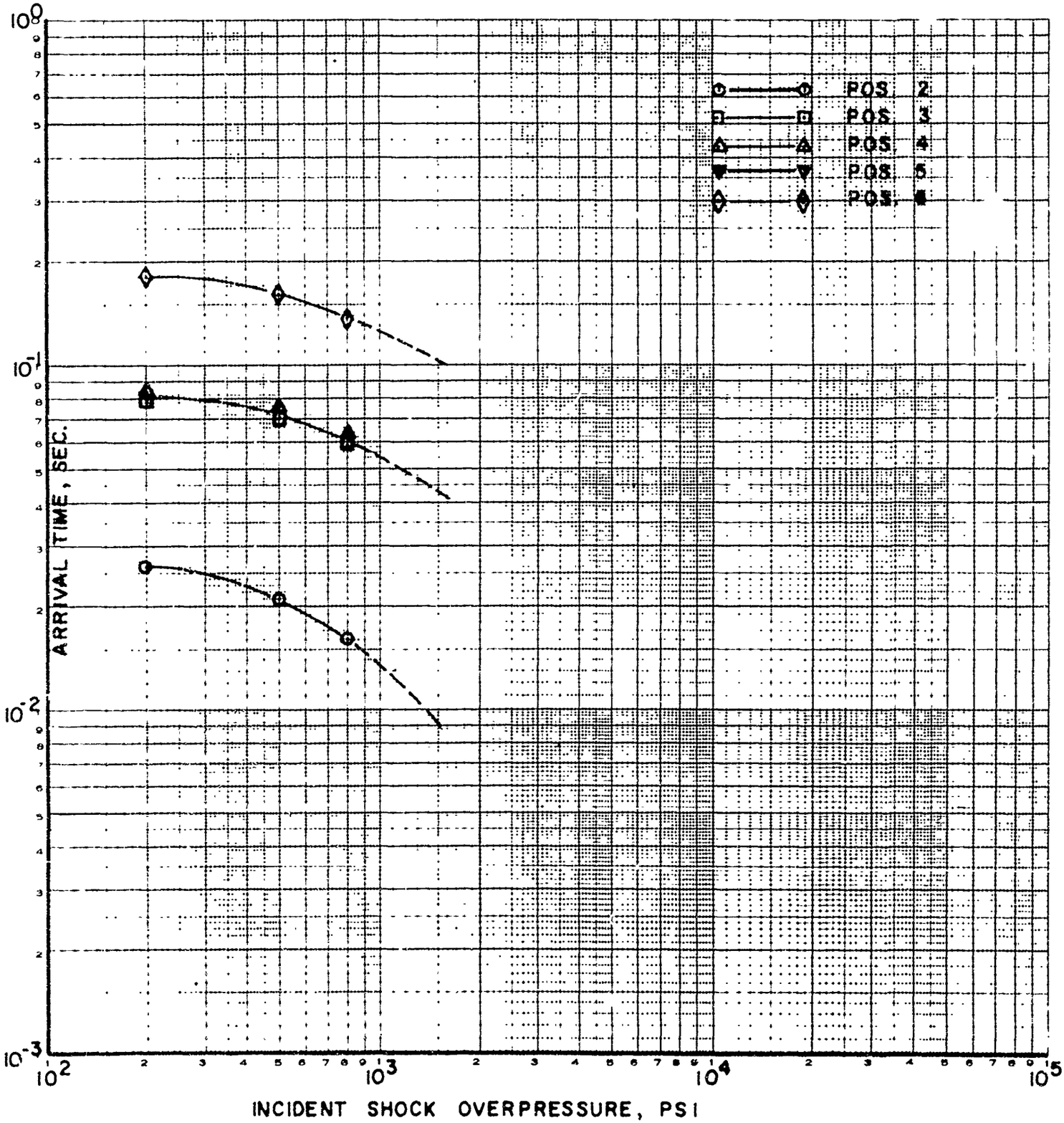

FIG. 28 - INCIDENT SHOCK OVERPRESSURE vs. TIME OF ARRIVAL OF TRANSMITTED SHOCK WAVE AT GAGE POSITIONS - MODEL # 2

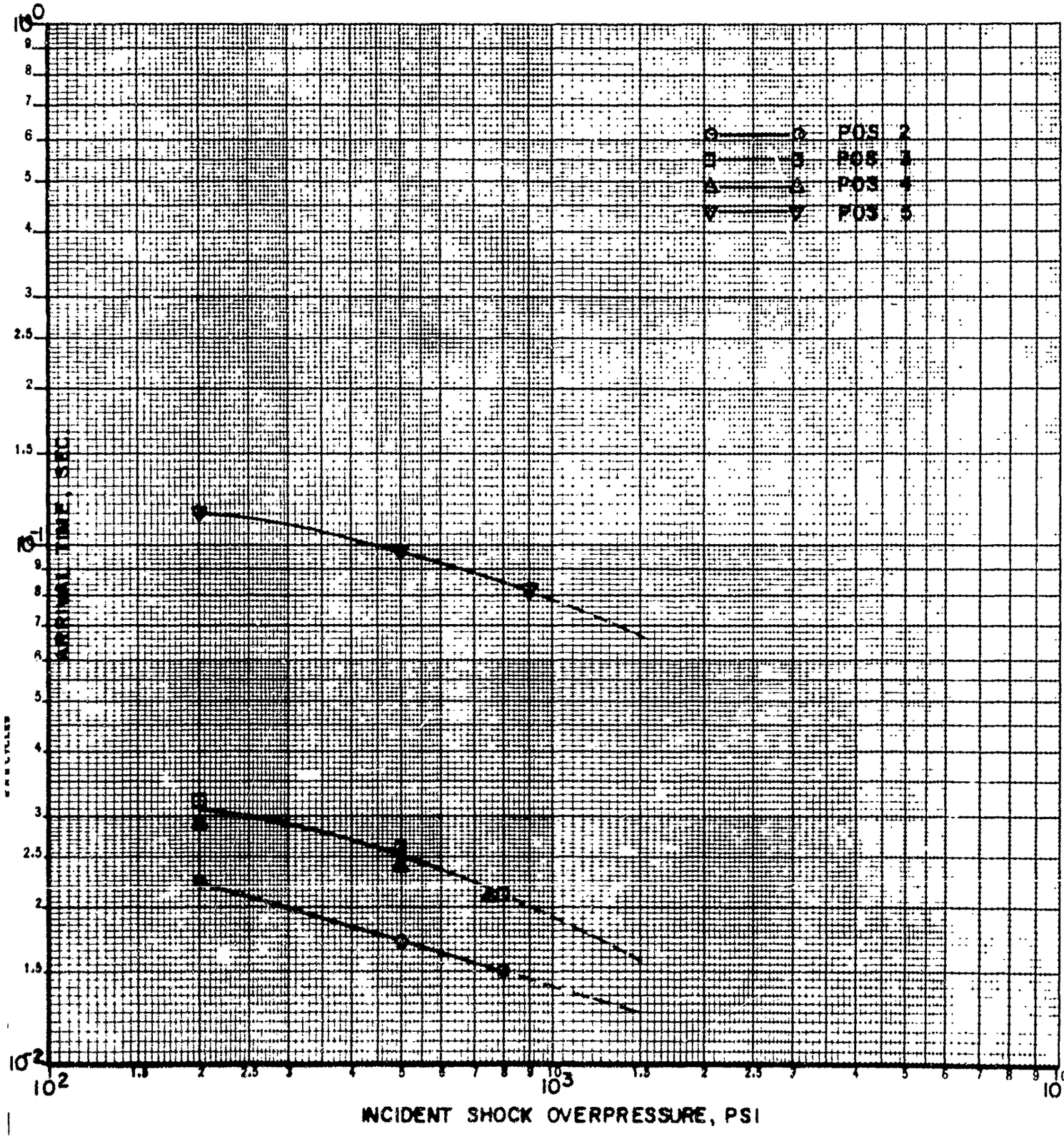

FIG. 29 — INCIDENT SHOCK OVERPRESSURE vs. TIME OF ARRIVAL OF TRANSMITTED SHOCK WAVE AT GAGE POSITIONS.
MODEL #3

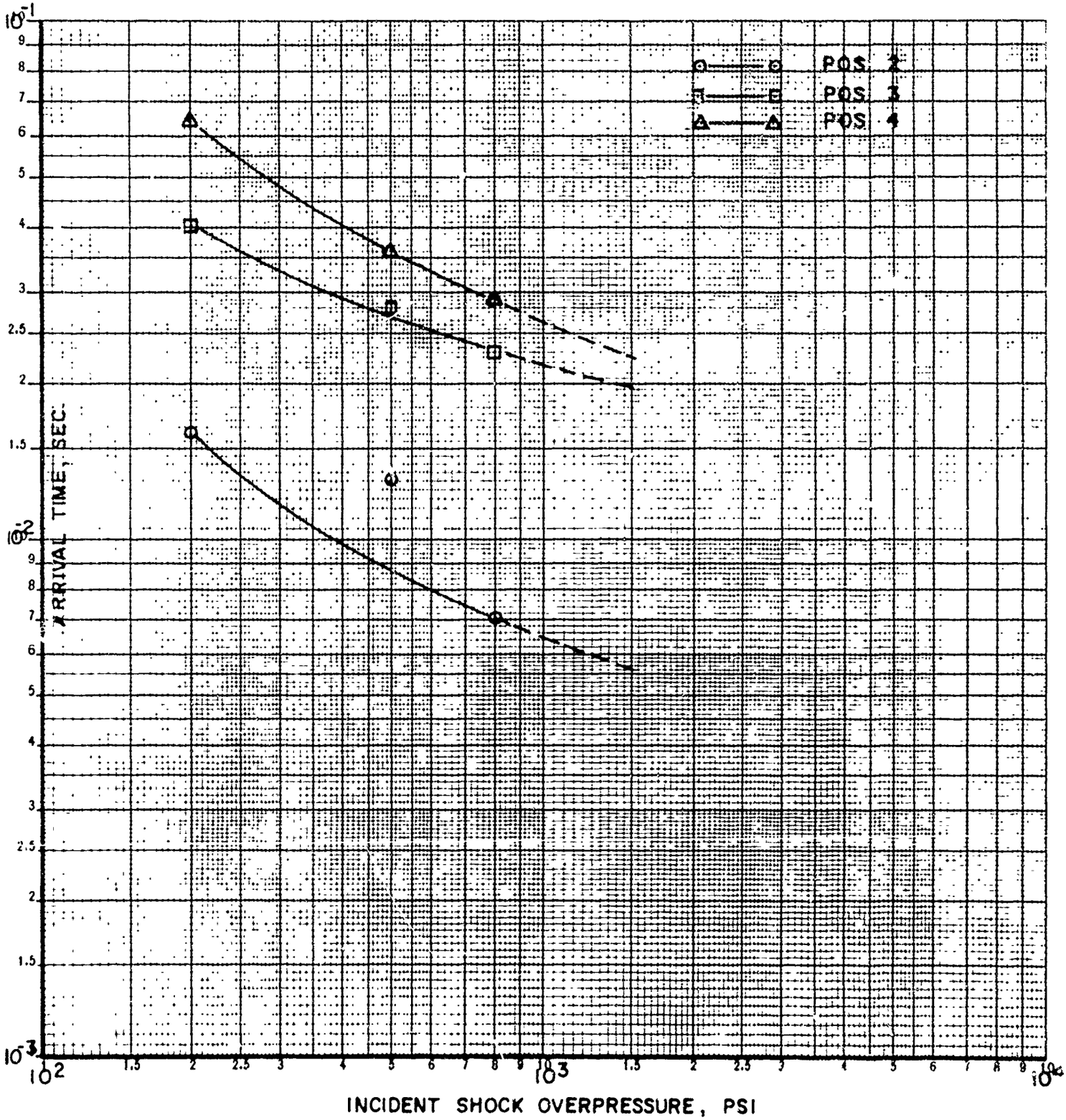

FIG. 30- INCIDENT SHOCK OVERPRESSURE vs. TIME OF ARRIVAL OF TRANSMITTED SHOCK WAVE AT GAGE POSITIONS.
MODEL # 4

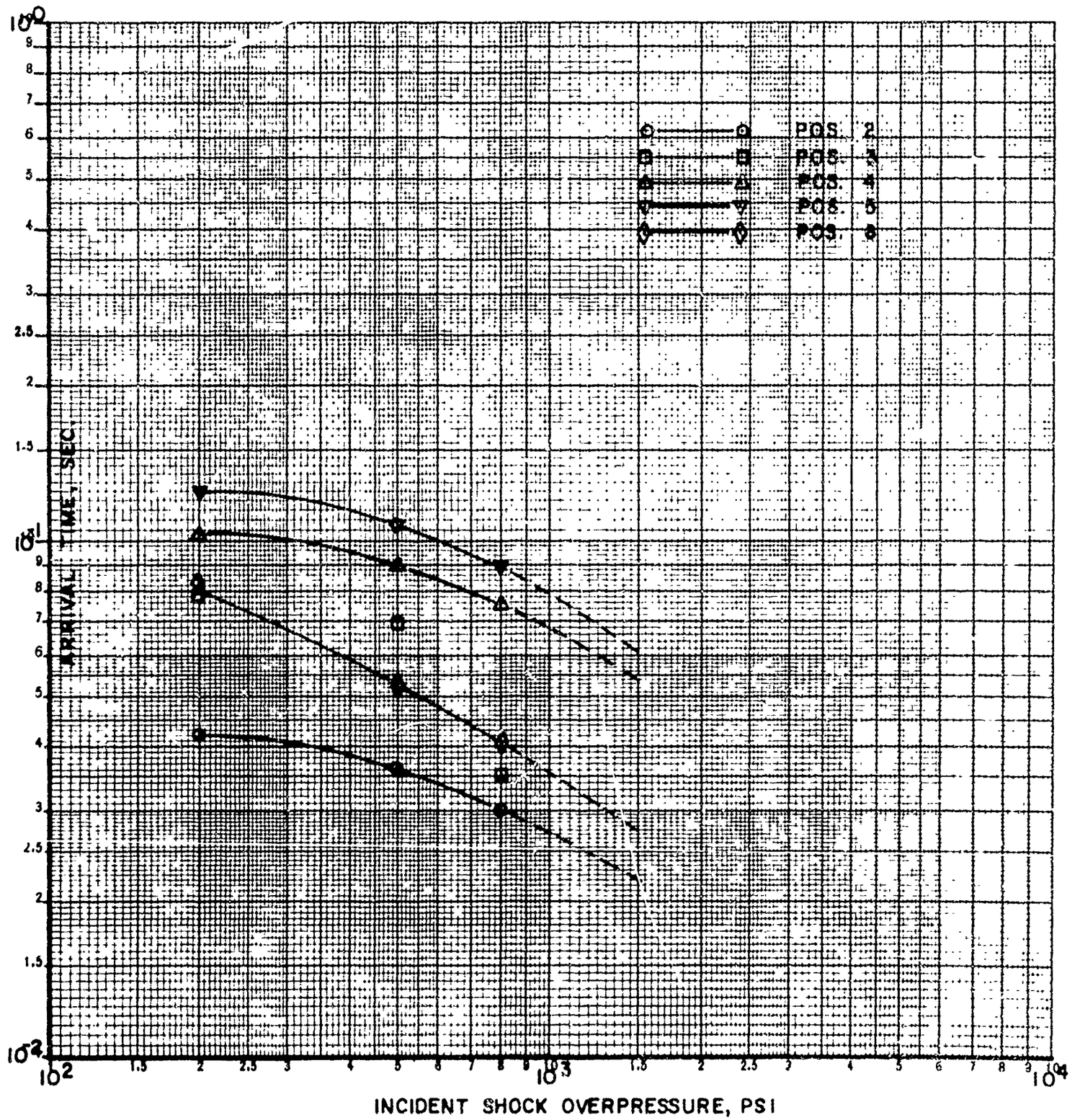

FIG. 31 - INCIDENT SHOCK OVERPRESSURE vs. TIME OF ARRIVAL OF RAREFACTION WAVE AT GAGE POSITIONS - MODEL #1

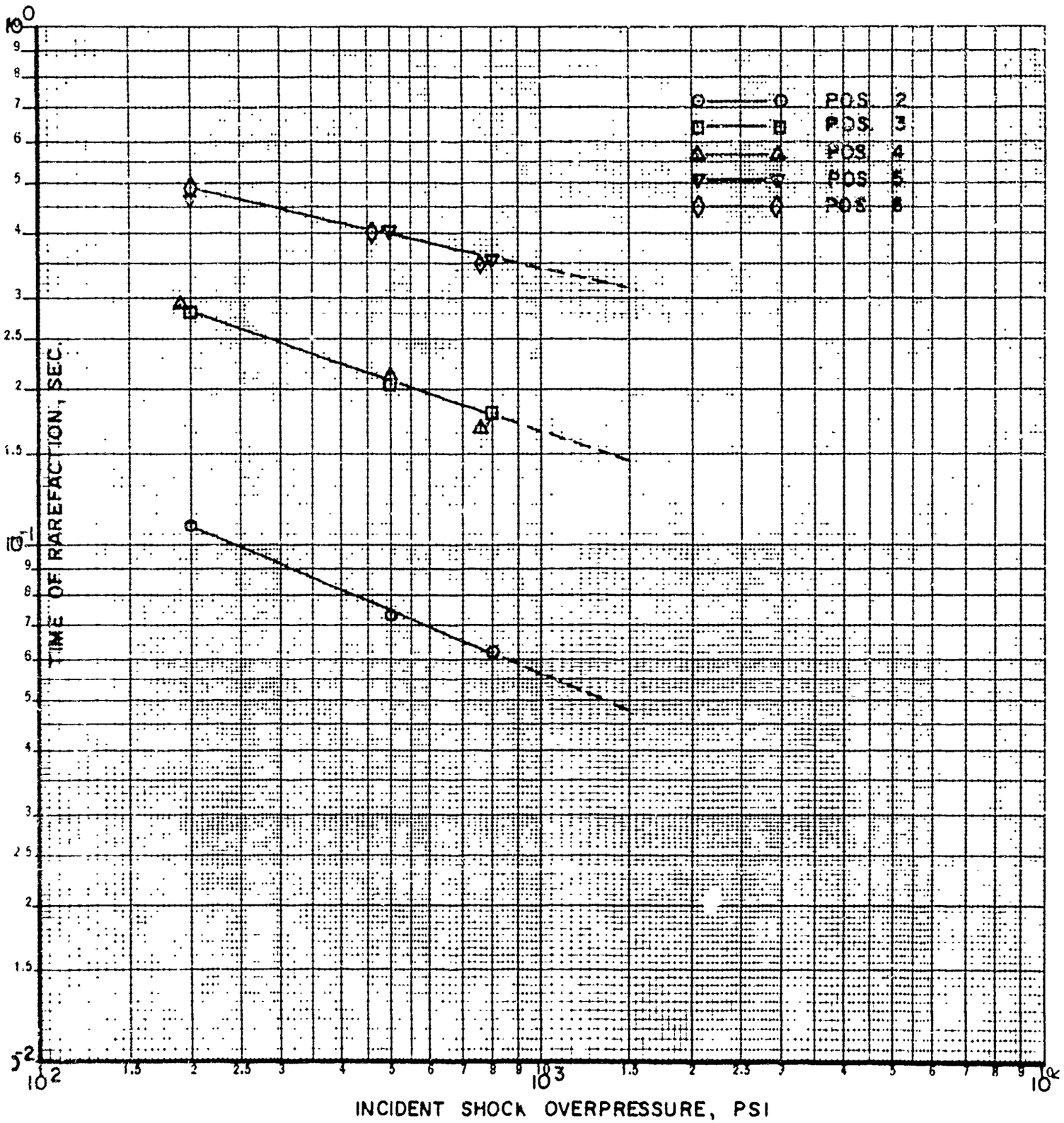

FIG. 32 – INCIDENT SHOCK OVERPRESSURE vs. TIME OF ARRIVAL OF RAREFACTION WAVE AT GAGE POSITIONS- MODEL #2

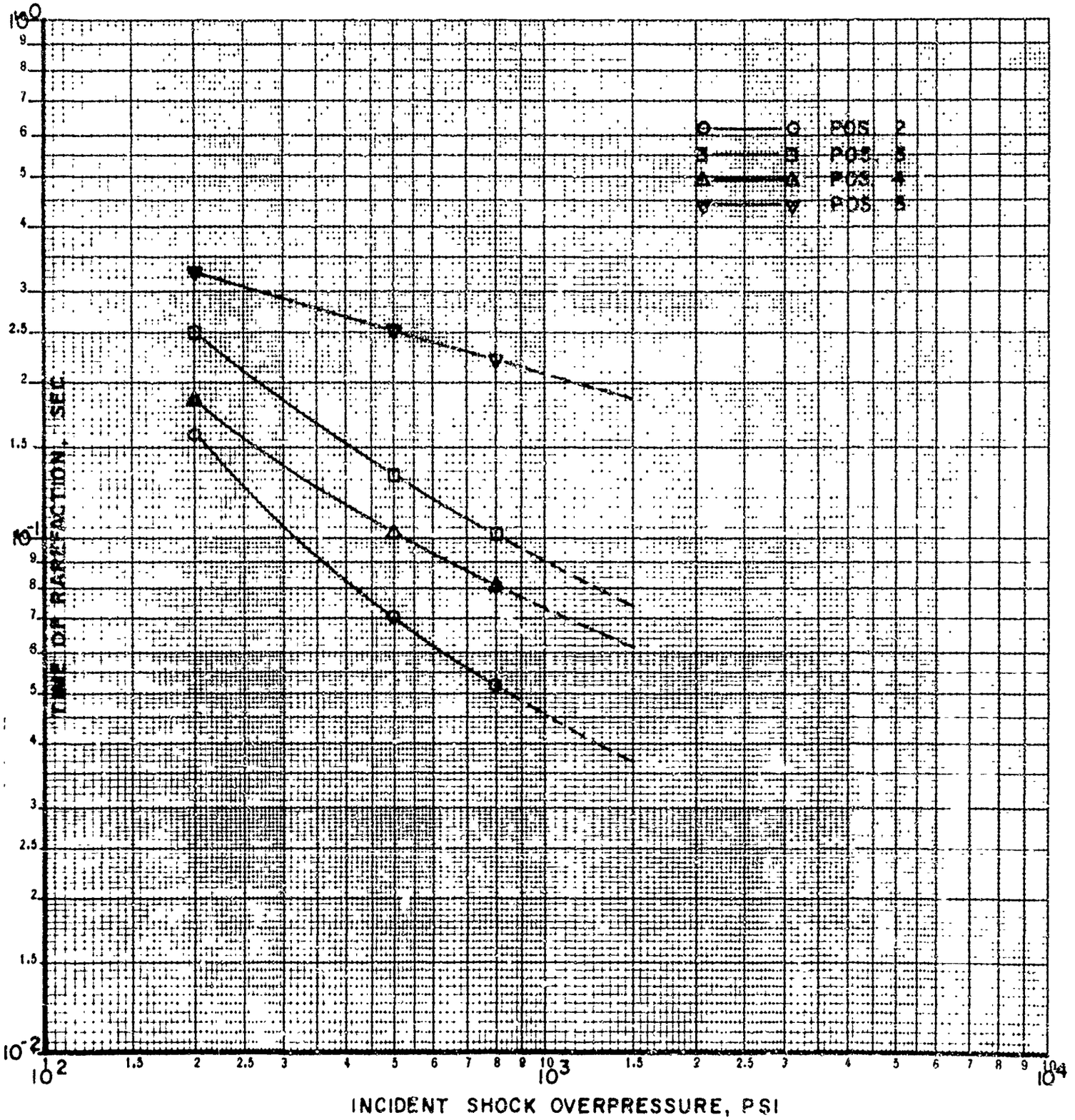

FIG. 33 – INCIDENT SHOCK OVERPRESSURE vs. TIME OF ARRIVAL OF RAREFACTION WAVE AT GAGE POSITIONS – MODEL #3

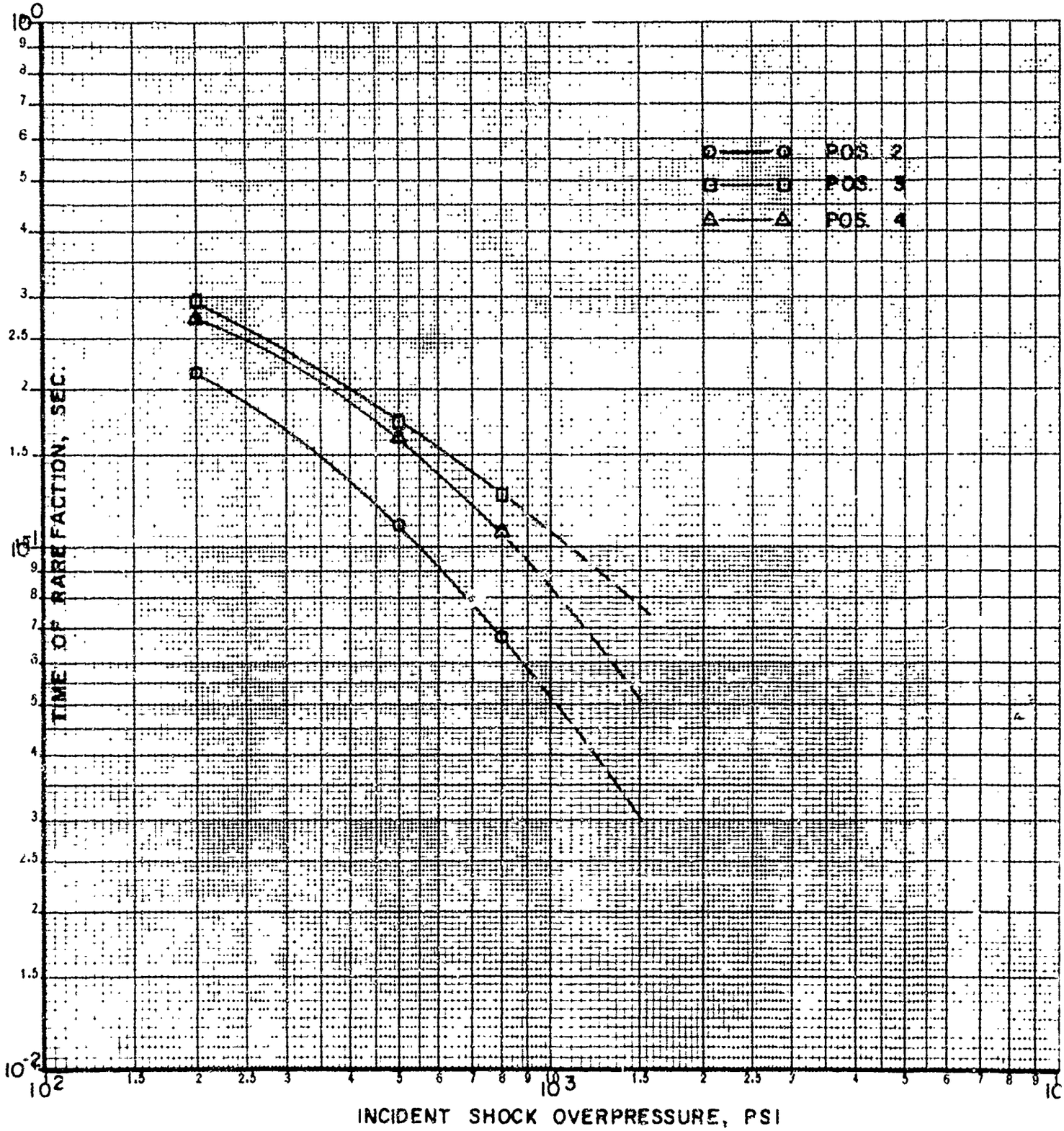

FIG. 34 - INCIDENT SHOCK OVERPRESSURE vs. TIME OF ARRIVAL OF RAREFACTION WAVE AT GAGE POSITIONS. MODEL #4

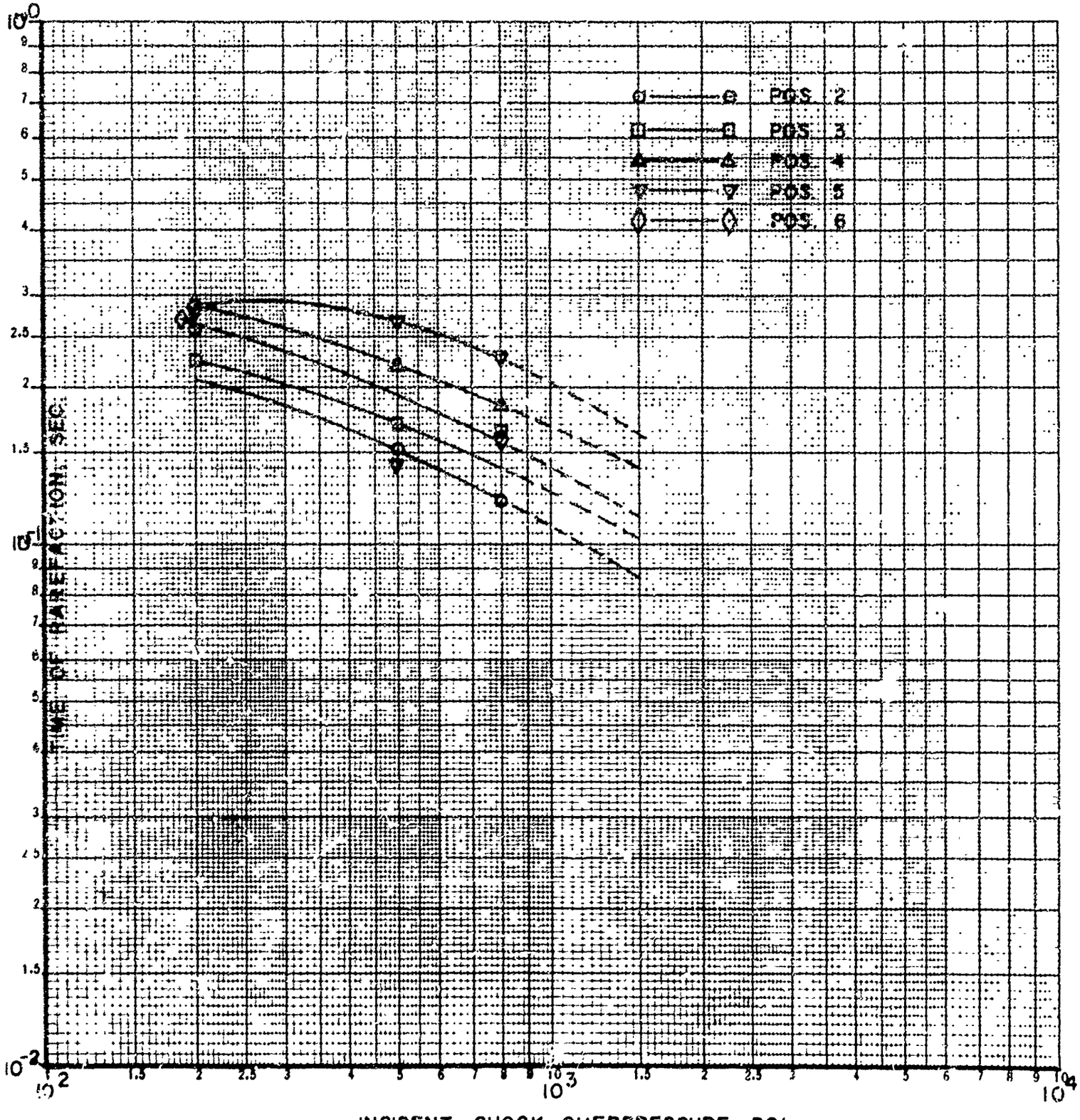

FIG. 35 – INCIDENT SHOCK OVERPRESSURE vs. TRANSMITTED OVER-PRESSURE AT TIME OF RAREFACTION AT GAGE POSITIONS.
MODEL #1

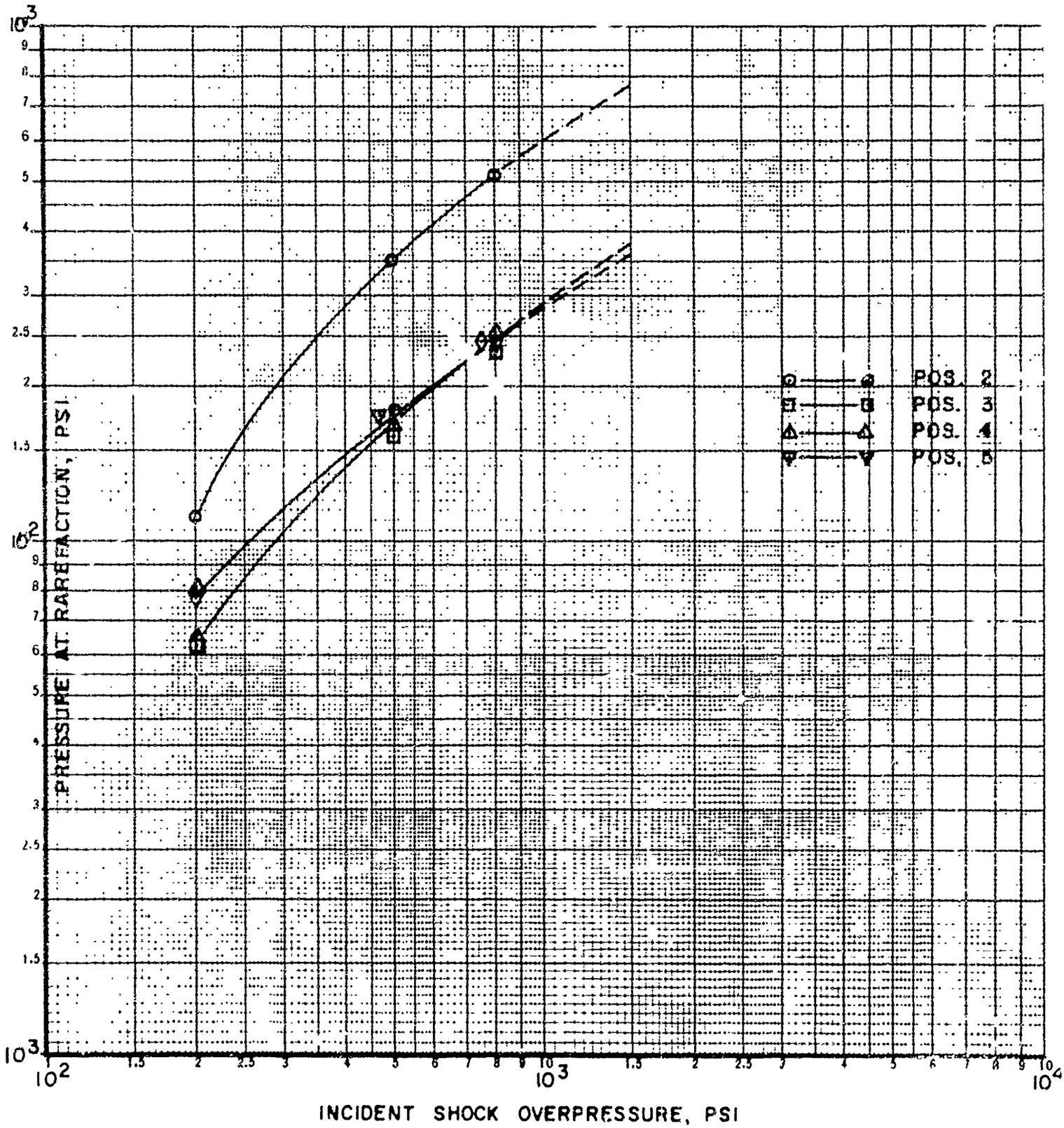

FIG. 36 – INCIDENT SHOCK OVERPRESSURE vs. TRANSMITTED OVER-PRESSURE AT TIME OF RAREFACTION AT GAGE POSITIONS. MODEL # 2

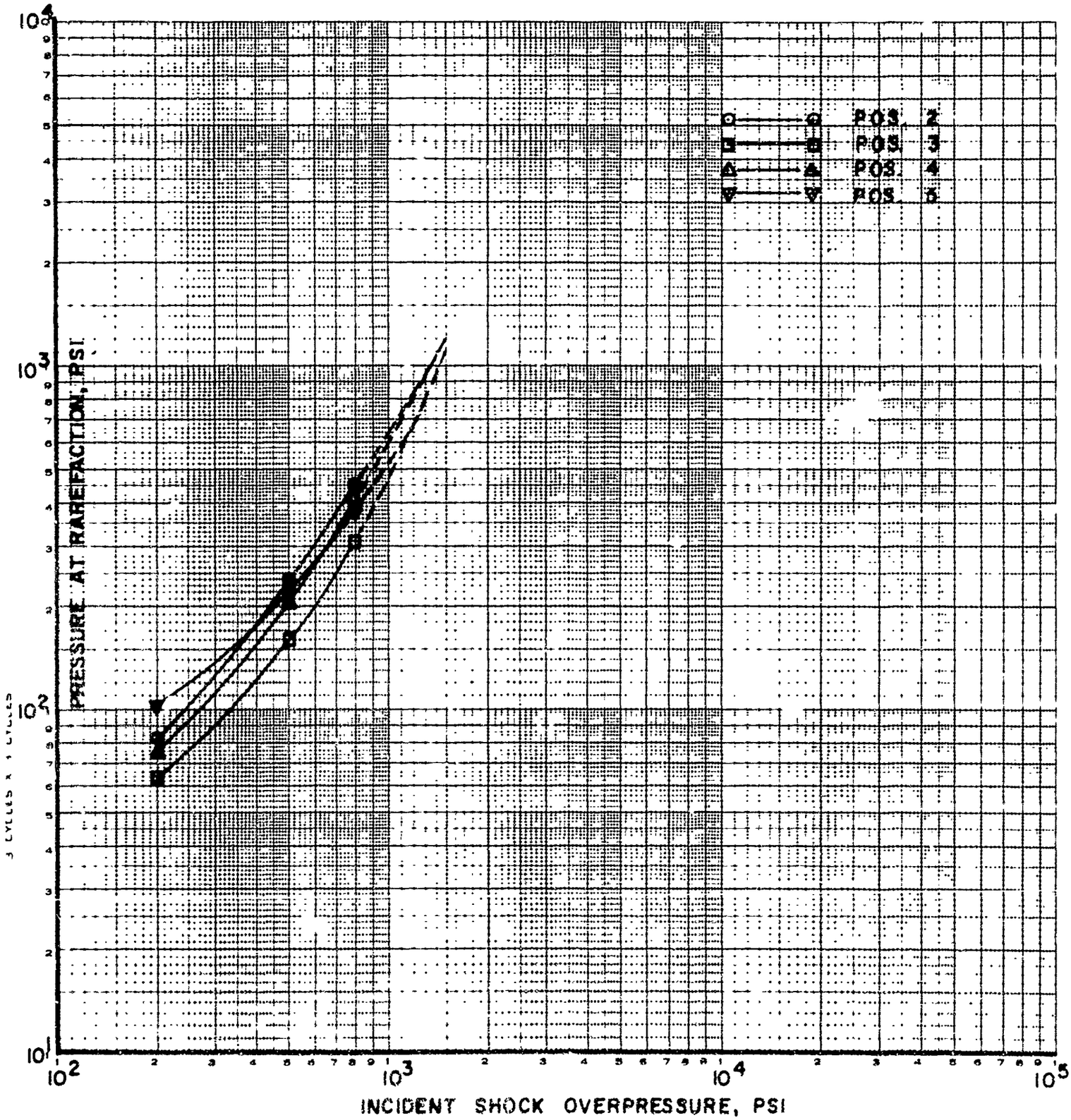

FIG. 37- INCIDENT SHOCK OVERPRESSURE vs. TRANSMITTED OVER-PRESSURE AT TIME OF RAREFACTION AT GAGE POSITIONS.
MODEL # 3

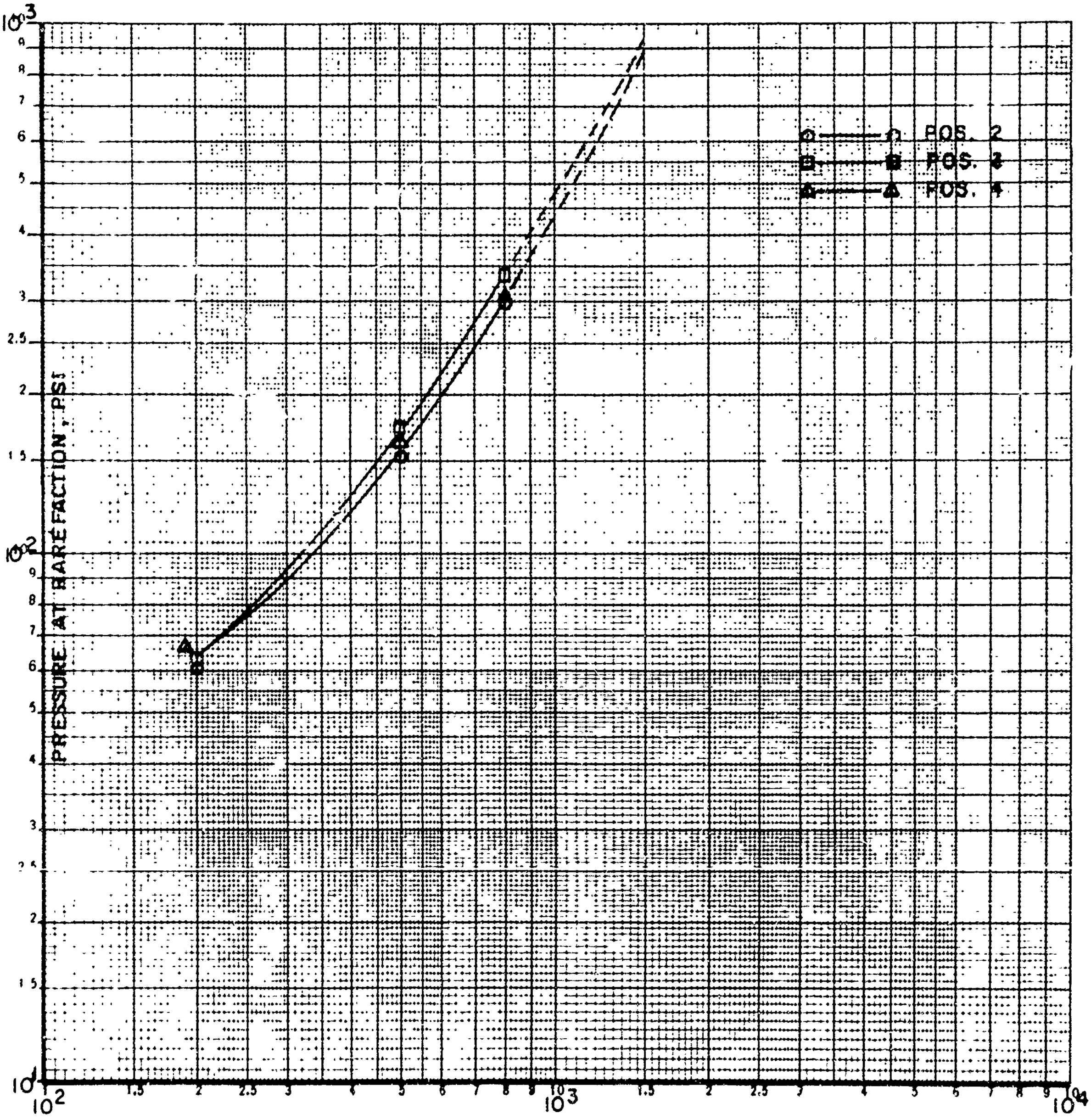

FIG. 38- INCIDENT SHOCK OVERPRESSURE vs. TRANSMITTED OVERPRESSURE AT TIME OF RAREFACTION AT GAGE POSITIONS. MODEL #4

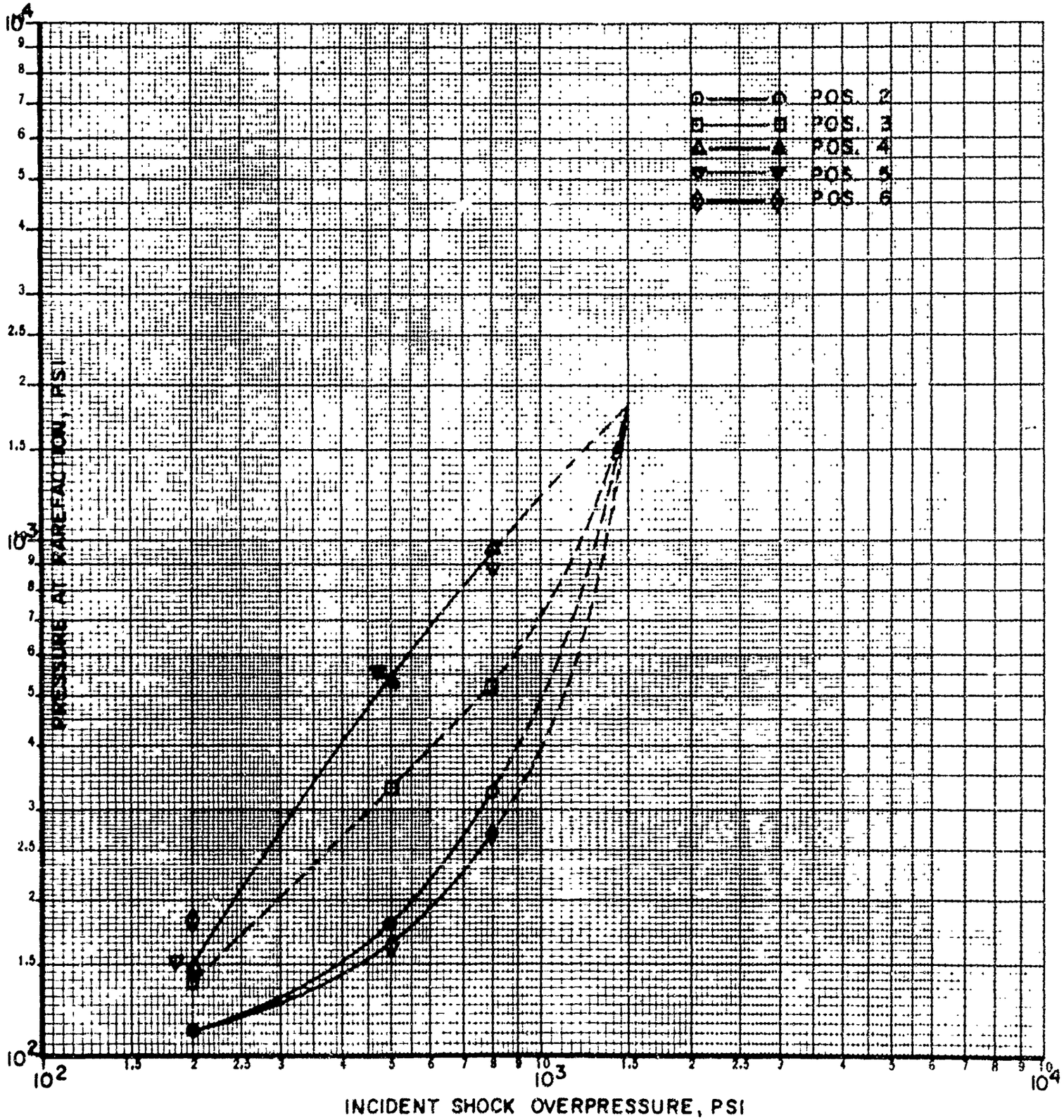

TABLE 1 - PRESSURE AND TIME VALUES

MODEL	POS	P_S	P_A	t_A	P_R	t_R	I_M	I_N
1	3	200	17	.026	122	.109	---	---
		500	24	.021	350	.073	[illegible]	[illegible]
		800	55	.016	515	.06[illegible]	---	---
		1500	950	.009	760	.04[illegible]	---	---
	4	200	16	.07[illegible]	62	.2[illegible]	[illegible]	[illegible]
		500	20	.071	163	.20[illegible]	[illegible]	[illegible]
		800	28	.059	233	.1[illegible]	[illegible]	---
		1500	72	.043	380	.145	---	---
	4	200	16	.083	64	.2[illegible]	---	---
		500	23	.075	170	.204	---	---
		800	34	.063	256	.176	---	---
		1500	72	.043	380	.145	---	---
	5	200	12	.177	77	.468	---	---
		500	19	.159	170	.407	---	---
		800	21	.133	245	.357	---	---
		1500	28	.101	365	.315	---	---
	6	200	27	.181	79	.484	---	---
		500	32	.161	178	.408	---	---
		800	57	.137	244	.358	---	---
		1500	950	.101	365	.315	---	---

TABLE 1 - PRESSURE AND TIME VALUES (CONT'D)

MODEL	POS	P_S	P_A	t_A	P_R	t_R	P_M	t_M
2	2	200	28	.022	82	.157	84	.085
		500	66	.017	235	.070	---	---
		800	91	.015	450	.054	---	---
		1500	132	.012	1200	.037	---	---
	3	200	23	.032	64	.250	57	.171
		500	34	.026	160	.134	160	.101
		800	50	.021	315	.103	317	.086
		1500	110	.016	1100	.074	---	---
	4	200	29	.029	76	.185	78	.124
		500	68	.024	205	.102	---	---
		800	111	.021	415	.081	---	---
		1500	188	.016	1200	.062	---	---
	5	200	49	.116	101	.323	101	.318
		500	91	.097	218	.252	217	.238
		800	92	.082	380	.221	---	---
		1500	150	.068	1100	.185	---	---
3	2	200	65	.016	61	.214	67	.033
		500	127	.013	153	.108	157	.050
		800	224	.007	297	.067	322	.045
		1500	690	.006	900	.030	1320	.056
	3	200	12	.040	64	.296	---	---
		500	27	.028	173	.171	---	---
		800	69	.023	333	.125	---	---
		1500	400	.020	925	.076	---	---
	4	200	45	.064	65	.272	---	---
		500	166	.036	165	.161	---	---
		800	279	.029	303	.106	---	---
		1500	515	.023	900	.052	---	---

TABLE 1 - PRESSURE AND TIME VALUES (CONT'D)

MODEL	POS	P_S	P_A	t_A	P_R	t_R	P_M	t_M
4	2	200	51	.042	111	.259	---	---
		500	55	.036	180	.150	---	---
		800	80	.030	325	.120	---	---
		1500	114	.022	1830	.086	---	---
	3	200	22	.078	140	.224	---	---
		500	174	.069	330	.170	---	---
		800	207	.03[illegible]	525	.162	---	---
		1500	242	.027	1830	.102	---	---
	4	200	76	.102	148	.287	---	---
		500	159	.089	538	.217	---	---
		800	393	.075	935	.185	---	---
		1500	3900	.054	1830	.140	---	---
	5	200	135	.124	147	.274	---	---
		500	926	.109	545	.267	---	---
		800	1495	.089	895	.229	---	---
		1500	1820	.061	1830	.160	---	---
	6	200	11	.081	184	.270	---	---
		500	34	.052	165	.142	---	---
		800	153	.041	270	.156	---	---
		1500	130	.027	1830	.112	---	---

P_S - Incident Shock Overpressure, PSI

P_A - Initial Transmitted Shock Overpressure, PSI

t_A - Time of Arrival of Transmitted Shock Wave, SEC.

P_R - Transmitted Overpressure at Time of Rarefaction, PSI

t_R - Time of Arrival of Rarefaction Wave, SEC.

P_M - Maximum Transmitted Overpressure, PSI

t_M - Time of Occurrence of Maximum Transmitted Overpressure, SEC.

DISTRIBUTION LIST

No. of Copies	Organization
1	Director Advanced Research Projects Agency ATTN: Dr. Charles Bates Washington, D. C. 20301
2	Chief, Defense Atomic Support Agency Washington, D. C. 20301
5	Commanding General Field Command Defense Atomic Support Agency Sandia Base P. O. Box 5100 Albuquerque, New Mexico
1	Director IDA/Weapon Systems Evaluation Group Room 1E875, The Pentagon Washington, D. C. 20315
1	Secretary of Defense Installations and Logistics ATTN: Mr. John T. Lynch Washington 25, D. C.
1	Commanding General U. S. Army Materiel Command ATTN: AMCRD-RP-B Washington, D. C. 20315
1	Commanding General U. S. Army Materiel Command ATTN: AMCRD-DN Washington, D. C. 20315
1	Commanding Officer Picatinny Arsenal ATTN: ORDBB-TK Dover, New Jersey 07801
1	Commanding General White Sands Missile Range ATTN: ORDBS-OM-W New Mexico 88002
1	Commanding Officer U. S. Army Chemical Warfare Labs ATTN: Technical Library Edgewood Arsenal, Maryland 21040
2	Chief of Engineers ATTN: ENGNB ENGEB Department of the Army Washington 25, D. C.
1	Commanding General U. S. Army Engineer Research and Development Laboratories ATTN: Chief, Technical Support Branch Fort Belvoir, Virginia 22060
1	Commanding General The Engineer Center ATTN: Asst. Commandant, Engineer School Fort Belvoir, Virginia 22060
1	Director Waterways Experiment Station ATTN: Library P. O. Box 631 Vicksburg, Mississippi
1	Commanding General U. S. Army Signal Research and Development Laboratory ATTN: Technical Documents Center, Evans Area Fort Monmouth, New Jersey 07703
1	Director of Special Weapons Development U. S. Continental Army Command ATTN: Chester I. Peterson Fort Bliss, Texas 79906
1	Chief of Research and Development ATTN: Atomic Division Department of the Army Washington 25, D. C.

DISTRIBUTION LIST

No. of Copies	Organization
1	Chief, Bureau of Naval Weapons ATTN: DLI-3 Department of the Navy Washington, D. C. 20360
3	Commander U. S. Naval Ordnance Laboratories ATTN: EA EU E White Oak Silver Spring 19, Maryland
1	Commander U. S. Naval Ordnance Test Station ATTN: E. A. Zeitlin, Code 45419 China Lake, California 93557
3	Chief, Bureau of Ships ATTN: Code 372 Code 423 Code 210L, Tech Lib Department of the Navy Washington, D. C. 20360
2	Chief, Bureau of Yards and Docks ATTN: D-400 D-440 Department of the Navy Washington, D. C. 20360
1	Chief of Naval Research ATTN: Code 811 Department of the Navy Washington, D. C. 20360
1	Commanding Officer and Director David W. Taylor Model Basin ATTN: Library, Code 042 Washington, D. C. 20007
1	Commanding Officer and Director U. S. Naval Civil Engineering Lab Port Hueneme, California
1	Commanding Officer and Director U. S. Naval Electronics Laboratory San Diego 52, California
2	AFSC (SCRWA, SCTWMB) Andrews Air Force Base Washington, D. C. 20331
3	APGC (PGAPI, PGTWR, PGTW) Eglin Air Force Base Florida 32542
1	RADC Griffiss Air Force Base New York 13442
1	AFWL (Tech Info Div) Kirtland Air Force Base New Mexico 87117
1	AFCRL (CRQST-2) L. G. Hanscom Field Bedford, Massachusetts 01731
8	Commander 4258 Systems Program Office ATTN: Maj. H. K. Christian L. G. Hanscom Field Bedford, Massachusetts 01731
1	BSD Norton Air Force Base California 92409
1	ASD (ASAPRL) Wright-Patterson Air Force Base Ohio 45433
1	Hq, USAF (AFOCE) Washington, D. C. 20330
1	Hq, USAF (AFRDC) Washington, D. C. 20330

DISTRIBUTION LIST

No. of Copies	Organization
1	Hq, USAF (AFCIN-3K2) Washington, D. C. 20330
1	Director National Aeronautics and Space Administration Langley Research Center ATTN: Mr. John Stack Langley Field, Virginia
1	Superintendent Eastern Experiment Station U. S. Bureau of Mines ATTN: Dr. Leonard Obert College Park, Maryland
1	U. S. Atomic Energy Commission Sandia Corporation P. O. Box 5800 Albuquerque, New Mexico 87115
1	President Sandia Corporation ATTN: Classified Document Division for M. L. Merritt Sandia Base Albuquerque, New Mexico
1	U. S. Atomic Energy Commission Los Alamos Scientific Laboratory ATTN: Reports Librarian for Dr. Alvin C. Graves P. O. Box 1663 Los Alamos, New Mexico
2	U. S. Atomic Energy Commission Classified Technical Library ATTN: Technical Information Service, For Mrs. Jean O'Leary, Dr. Paul C. Fine Washington, D. C. 20545
1	Bell Telephone Laboratories, Inc. ATTN: Mr. T. Gressitt Whippany, New Jersey
1	The Boeing Company ATTN: Mr. R. H. Carlson Seattle, Washington
1	General American Transportation Company ATTN: Mr. T. G. Morrison 7501 North Natchez Avenue Niles 48, Illinois
1	Space Technology Laboratories, Inc. ATTN: Mr. J. Halsey 5500 West El Segunda Blvd. Los Angeles, California
1	Illinois Institute of Technology ATTN: Dr. Eugene Sevin Chicago, Illinois 60616
1	Dr. Walker Bleakney Palmer Physical Laboratory Princeton University Princeton, New Jersey
1	Dr. Robert Hansen Massachusetts Institute of Technology Division of Industrial Cooperation 77 Massachusetts Avenue Cambridge, Massachusetts
1	Dr. Bruce G. Johnston The University of Michigan University Research Security Office Lobby 1, East Engineering Bldg. Ann Arbor, Michigan 48104
1	Dr. Carl Kisslinger St. Louis University St. Louis, Missouri

DISTRIBUTION LIST

No. of Copies	Organization
1	Dr. Nathan M. Newmark University of Illinois Talbot Laboratory, Room 207 Urbana, Illinois
	Aberdeen Proving Ground
	Chief, TIB
	Air Force Liaison Office Marine Corps Liaison Office Navy Liaison Office CDC Liaison Office
	D&PS Branch Library